

ABSTRACT

VOELLER, SARAH KATHERINE. Using GIS to Reassociate Commingled Remains. (Under the Direction of Dr. Ann H. Ross).

Commingled remains can result from a natural disaster or a large scale accident such as a plane crash, however, more frequently commingling is observed in mass graves, related to crimes against humanity. To dispose of evidence quickly perpetrators bury bodies together in mass graves. Commingling in a mass grave can happen naturally as bodies decompose and lose soft tissue that associates body parts and bones. It is exacerbated when one grave is added to another, when remains are intentionally damaged or when a grave is relocated. Commingled remains prohibit investigators from making identifications and repatriating complete bodies back to families. Methods have been created to address commingling; however, some are costly while others are time consuming. The most commonly employed methods include: visual pair matching, articulation, taphonomic comparison, age, osteometric sorting and DNA analysis. The application of methods is also case specific. For example, using DNA is useless when remains have been burned and visual methods do not work well if the decedents were of similar ancestry, sex and age. When remains are in situ, as is the case when a mass grave is found, contextual information can aid in the reassociate process. Elements are often collected as one body because an investigator noticed that they were spatially associated. The laws of spatial analysis dictate that objects that are close to each other in space are most likely associated.

This research expands upon the laws of spatial analysis in order to test the hypothesis that a disarticulated skeletal element in closest proximity to a corresponding element is most likely associated with that element. A skeletal commingling was recreated using ten domestic pigs in a mass grave at the North Carolina State University Lake Wheeler Field

Site. The pigs chosen were of various sizes and pigs of similar size were placed at opposite sides of the grave aid in control. Time lapse photography was also used to track the movement of bones over time. The provenience of skeletal elements was mapped using a total station. Bones were mapped on articular surfaces, sometimes two or three measurements per bone, so previously articulated elements could be identified. Total station data were loaded into ArcGIS 10.2 and spatial relationships were analyzed. Near 3D ® was used to find the closest missing element of an unassociated bone. This tool finds the closest points from one data set to the points in another data set. Points were separated by bone type, side and articular surface to create a total of 34 data sets. One data set would consist of all left proximal humerus points, for example. The Near 3D analysis reassociated skeletal elements in 91.89% of cases. Because small bones such as phalanges, carpals, metapodials, ribs, and vertebrae could not be identified precisely by type they were not included in the Near 3D analysis. However, clusters of associated small bones were identified using Hot Spot Analysis ®. A total of 75.22% of small bones were spatially clustered. Osteometric sorting, a statistical reassociation method was also employed and compared to the Near 3D analysis. The Near 3D analysis reassociated remains 43.72% more often than osteometric sorting. This research highlights the importance of documenting contextual relationships and serves as a protocol for mapping skeletal elements in a mass grave and reassociating them in a GIS. Spatial analysis should be employed at first order and then followed by other methods. This will reduce the number of comparisons that need to be made with osteometric sorting or visual pair matching, which will hasten the reassociation process.

Using GIS to Reassociate Commingled Remains

by
Sarah Katherine Voeller

A thesis submitted to the Graduate Faculty of
North Carolina State University
in partial fulfillment of the
requirements for the degree of
Master of Arts

Anthropology

Raleigh, North Carolina

2015

APPROVED BY:

Dr. Wes Watson

Dr. Heather Cheshire

Dr. Ann Ross
Committee Chair

DEDICATION

This thesis is dedicated to my family who encouraged and supported me throughout my education.

BIOGRAPHY

Sarah Voeller attended the University of Central Florida where she completed her Bachelor of Arts in Anthropology. Subsequently, she attended the Archaeological Field School at James Madison's Montpelier in Virginia where she developed an interest in Archaeology. As a volunteer at the local Medical Examiner's office she cultivated an interest in forensic science that she pursued as a graduate student. She completed graduate school at North Carolina State University with a Master of Arts in Anthropology and a Graduate Certificate and GIS. Having finished graduate school she hopes to find a career in which she can apply her skills in forensic science, archaeology and GIS.

ACKNOWLEDGEMENTS

I would like to thank my advisor Dr. Ann Ross for guiding me throughout the implementation of this research. She encouraged me when I chose this topic and supported me throughout the process. Thank you to Dr. Wes Watson, who assisted in acquiring and placing the pigs in the grave and Steve Denning who built the protective cage in the summer heat. Thank you to Gary Knight who created an amazing photography system that was instrumental to this project.

I would like to acknowledge all those who assisted with mapping of the grave. Thank you to my cohort and new class mates, who operated the total station, held the prism, bagged pig bones and recorded points in spite of their busy schedules during the fall semester. Thank you to Andy for mapping the second half of the grave with me on the weekends. I truly could not have completed this project without your help.

I am also grateful to my sister Megan who has proofread countless papers for me throughout my college endeavors and helped me grow as a person and writer. You always guide me and I could not have completed graduate school without your constant encouragement.

TABLE OF CONTENTS

LIST OF TABLES	vii
LIST OF FIGURES	viii
CHAPTER 1: Introduction	1
CHAPTER 2: Review of the Literature	4
I. Human Rights Violations	4
II. Commingling	10
III. Taphonomy	14
IV. Geographic Information Systems (GIS)	15
V. Total Station Survey and Mapping	18
VI. Studies Incorporating GIS into the Analysis of Human Remains	23
CHAPTER 3: Materials and Methods	25
I. Using Pigs as a Proxy for Humans	25
II. The Research Field Site	26
III. Sokkia SET 10 Total Station: Protocol for Set Up	30
IV. Time Lapse Photography and Aerial Photographs	30
V. Excavation	32
VI. Reassociation Using GIS	39
VII. Methods for Control	41
CHAPTER 4: Results	46
I. Results for Reassociations using GIS	46
II. Results for Osteometric Sorting	54
CHAPTER 5: Discussion	56
I. Reassociations made with GIS	56
II. Comparison of Methods: Osteometric Sorting	60

III. The Mapping Process	62
IV. Limitations	65
CHAPTER 6: Conclusion	68
LITERATURE CITED	71
APPENDIX	80
APPENDIX 1: Results for Near 3D and Osteometric Sorting.....	81

LIST OF TABLES

Table 3.1: Back Site Coordinates (in meters)	33
Table 3.2: 2 nd Fixed Point Coordinates (in meters)	33
Table 3.3: Bone Codes	35
Table 4.1: Results for Spatial Reassociation of Left Humeri and Radii	49
Table 4.2: Overall Results	49
Table 4.3: Results for Hot Spot Analysis of Vertebrae	53
Table 4.4: Results for Hot Spot Analysis of Ribs	54
Table 4.5: Results for Osteometric Sorting	55
Table 5.1: Quantified Results	59
Table 5.2: R ² Values for Each Regression Equation	61
Table 5.3: Suggested Codes	64
Table 7.1: Left Humerus and Radius	81
Table 7.2: Left Scapula and Humerus	82
Table 7.3: Right Scapula and Humerus	82
Table 7.4: Left Ulna and Humerus	83
Table 7.5: Right Ulna and Humerus	83
Table 7.6: Left Femur and Tibia (matched in columns by tibia)	84
Table 7.7: Right Femur and Tibia	84
Table 7.8: Left Tibia and Fibula	85
Table 7.9: Right Tibia and Fibula	85
Table 7.10: Right Talus and Calcaneus	86
Table 7.11: Left Talus and Calcaneus	86

Table 7.12: Left Tibia and Talus	87
Table 7.13: Right Tibia and Talus	87
Table 7.14: Left Femur and Ilium	88
Table 7.15: Right Femur and Ilium	88

LIST OF FIGURES

Figure 2.1: Mass Grave Sites in Rwanda	6
Figure 2.2: Crime Scene Map Created Using Total Station Points	18
Figure 2.3: Using the Total Station	20
Figure 3.1: The Lake Wheeler Field Site Being Renovated	27
Figure 3.2: Total Station Points Referenced to a Vertical Photograph.....	28
Figure 3.3: Cage Built to Protect the Remains from Scavengers	29
Figure 3.4: Camera Set Up	32
Figure 3.5: The Grave Mapped in 6 Meter x Meter Units	36
Figure 3.6: The Long Prism must be Operated by Two People	37
Figure 3.7: The Smaller Prism can be Operated by One Person	37
Figure 3.8: Visual Matching Based on Morphological Similarities	44
Figure 3.9: The Position of Bones in the Grave	45
Figure 4.1: Individuated Skeletal Elements	47
Figure 4.2: Individuated Skeletal Elements Referenced to a Photo	47
Figure 4.3: Rank of Correct Matches	49
Figure 4.4: Colors that Represent Hot and Cold Cells	50
Figure 4.5: Hot Spot Analysis of Phalanges	51
Figure 4.6: Hot Spot Analysis of Carpals	51
Figure 4.7: Hot Spot Analysis of Vertebrae	52
Figure 4.8: Hot Spot Analysis of Ribs	52
Figure 4.9: Hot Spot Analysis of Metapodials	53
Figure 5.1: A Map of the Mass Grave Created in GRASS	67

CHAPTER 1: Introduction

Human Rights have been defined by the United Nations (UN) in 30 distinct articles that guide humanitarian law (UN, 1948). There are 193 countries that are members of the UN and have sworn to uphold this law (Iqbal, 2012). Unfortunately, this has proved a difficult task. Humanitarian law has strong moral but weak legal force. Across the globe many countries suffer human rights violations in the form of genocide, forced disappearances and war crimes among other offenses (Neuffer, 1999; Verwimp, 2004; Perechocky, 2014). Such violations often result in high death tolls and mass graves containing the victims. Following these atrocities, truth commissions and criminal tribunals attempt to reconcile communities and bring justice to victims (Sarkin, 1999; Mettraux, 2005). These commissions and tribunals often enlist the help of forensic specialists in the investigation of mass graves. Specialists such as anthropologists and archaeologists collect evidence for court prosecutions and attempt to identify human remains in order to repatriate loved ones to family members (Steadman & Haglund, 2005; Crossland, 2013). Exhumations (disinterment of remains) and identification efforts have been growing since the late 80s and early 90s with the creation of groups like the Argentinian Forensic Anthropology Team (EAAF) and Physicians for Human Rights (PHR) (Snow et al., 1984; Steadman & Haglund, 2005).

A mass grave investigation is never straight forward and challenges are often present. After victims are interred in mass graves taphonomic processes follow that can confound investigations. These processes include environmental conditions, animal activity, and

human activity (Ubelaker, 1997). While anthropologists can determine the effects of environment and animal activity, human tampering is more problematic. Offenders may attempt to burn or disarticulate victims in order to prevent identification. Also, graves are often relocated or combined in an effort to keep evidence hidden (Haglund & Sorg, 1997).

These activities typically cause commingling or the mixing together of individuals. Commingling poses problems for identification, collection of evidence for criminal prosecution and repatriation in a timely manner (Ubelaker, 2008). The less complete a body, the less information the anthropologist has for identification and crime analysis. There are various methods available to address this problem including: morphological techniques, mathematical and statistical models, X-ray, fluorescence, molecular analysis and chemical analysis (Snow & Folk 1970; Eyman, 1965; McKern, 1958; Fulton et al., 1986; Finnegan & Chauduri 1990). However, the most commonly employed are DNA or morphological methods that detect size, shape, age, sex and similarities or differences among bilateral elements (Holland et.al. 1994; Buikstra et al. 1980; Adams & Konigsberg, 2004; Byrd, 2003; L'Abbe 2005; Owsley et al., 1995). While these techniques are effective, some are costly and others are time consuming. A recent study investigated the efficacy of reassociating commingled body parts with spatial analysis (Tuller et al., 2008). In this project the provenience of every body part in the grave was mapped with a total station. These data were then used to reassociate body parts based on proximity. This approach resulted in an 88% success rate when applied to a mass grave composed of primary and secondary interments. While this study served to show the utility of spatial analysis in a mass grave

setting, further exploration of this method would serve to delineate the scenarios when the method would be most useful, assess error and create a replicable protocol.

The purpose of this research is to investigate a method to reassociate commingled remains that is low cost and time efficient. Under the assumption that objects that are close to each other in space are most likely related, this research will test the hypothesis that a disarticulated skeletal element in closest proximity to a corresponding element is most likely associated with that element. A mass grave scenario was reproduced using domestic pigs. Provenience of elements was taken with a total station. Spatial analysis was used as the primary tool for reassociation of individuals. It is unclear how accurate this method will be for mapping elements that are within centimeters or millimeters of each other. The study will serve to create a protocol for spatial analysis, delineate appropriate application and assess the potential error of the method. A secondary goal of this research is to display the utility of GIS databases for documenting and analyzing crime scenes in general.

CHAPTER 2: A Review of the Literature

I. Human Rights Violations

The inspiration behind the 30 articles that make up the Declaration of Human Rights is that all human life should be valued equally and not wasted carelessly, as it has been in the past, with specific reference to World War II (Robinson, 1998). It is often difficult to discern at what point the line is drawn between cultural practice and a violation of human rights, or if anyone outside of a given culture is even in place to draw that line. But it is no question that these rights are to be respected by all countries that are part of the UN. “Everyone is entitled to all the rights and freedoms set forth in this Declaration, without distinction of any kind, such as race, color, sex, language, religion, political or other opinion, national or social origin, property, birth or other status”- Article 2. “Everyone has the right to life liberty and security of person”- Article 3. “Everyone has the right to freedom of opinion and expression”- Article 19, (UN, 1948). Unfortunately, violations of many of these articles are committed in countries that have signed the declaration promising to secure human rights for its people. These violations are often in the form of rape, slavery, forced disappearances, or genocide among others. The UN defines genocide as "acts committed with intent to destroy, in whole or in part, a national, ethnical, racial or religious group" (UN, 1948). Forced disappearances are defined as “persons who are arrested, detained or abducted against their will...by officials of different branches of the government...followed by refusal to disclose the fate or whereabouts of the person or a refusal to acknowledge the deprivation of their liberty” (UN, 1992). Both genocide and forced disappearances typically create high death

tolls. This produces the need to dispose of a large number of bodies. It is estimated that the Bosnian genocide resulted in 200,000 deaths while the genocide in Rwanda resulted in 800,000 deaths (Blum et al., 2008). Many of these bodies were disposed of in mass graves. Numerous mass grave sites have been identified in Rwanda (See Figure 2.1). As of 2000, 39 mass graves have been identified and 22 more sites are suspected in Bosnia (ICTY, 2000). In Argentina, the period of military rule (1974-1983) ended with about 9,000 missing individuals as a result of forced disappearances. In the following years 19 mass graves were found in Buenos Aires and many more in other provinces (EAAF, 2007). Similar situations of forced disappearances in Mexico and genocide in Cerska, Bosnia-Herzegovina exist (Human Rights Watch, 2013; Neuffer, 1999).

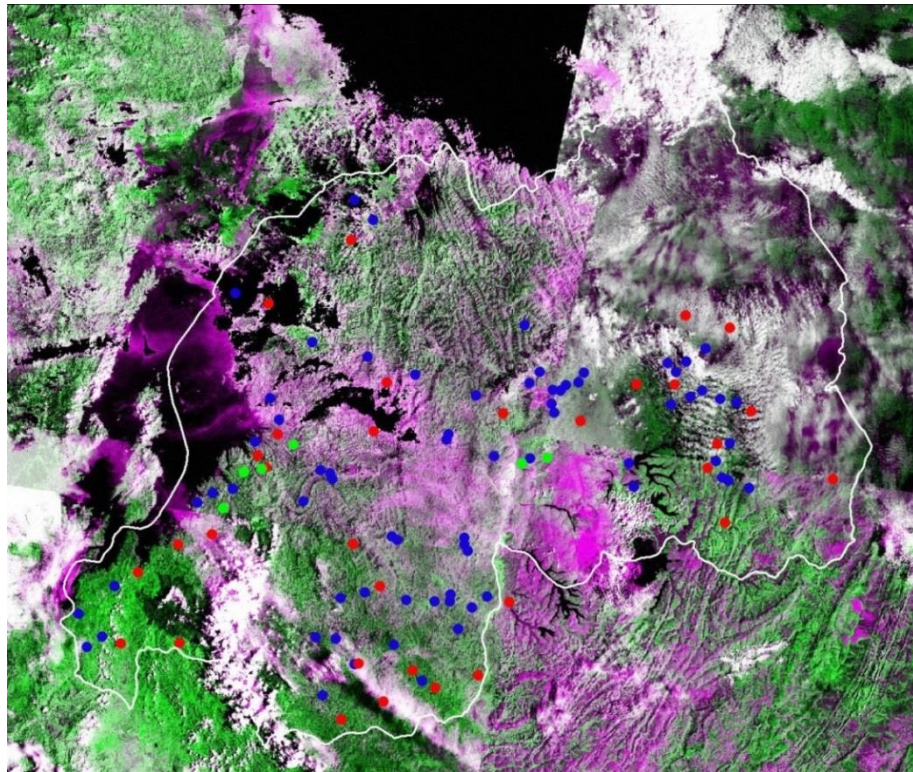


Figure 2.1: Mass Grave Sites in Rwanda. Mass graves are shown in blue, memorials are shown in red and resistance sites are shown in green (Yale University, 2010).

In response to these human rights violations truth commissions are often created. These commissions are fact finding bodies that create a conclusive record of the human rights abuses that occurred (Sarkin, 1999). They are established outside of ordinary law enforcement in order to remain unbiased. Their goal is to enlighten the public about what truly happened; healing and reconciliation are promoted over retributive justice (Rotberg & Thompson, 2010). Examples of this would be the Commission on Truth for El Salvador that was established to investigate war crimes after a civil war between the Salvadorian government and five leftist insurgent groups or the National Commission on the Disappeared that was established in Argentina to investigate forced disappearances conducted by the

military regime (Buergenthal, 1994; Perechocky, 2014). In other circumstances, retribution is sought through criminal tribunals. Criminal tribunals that serve as courts for the specific event have been created by the UN Security Council. The International Criminal Tribunal for Rwanda and the International Criminal Tribunal for the former Yugoslavia are notable examples (Mettraux, 2005). Trials can be held by these tribunals, local courts or the International Criminal Court (ICC) which was created in 1998 to impugn perpetrators of genocide, crimes against humanity and war crimes (UN, 1998). Truth Commissions, Criminal Tribunals and Non-government organizations (NGOs) commonly enlist the help of forensic specialists such as anthropologists and archaeologists to exhume and identify bodies that have been buried in mass graves (Steadman & Haglund, 2005; Crossland, 2013). Identified remains can be given back to families so a proper burial can be arranged for their loved one. Groups of forensic specialists that respond to these requests include NGOs such as the Argentinian Forensic Anthropology Team (EAAF), the Guatemalan Forensic Anthropology Foundation (FAFG), Physicians for Human Rights (PHR) and private organizations such as the International Committee of the Red Cross (ICRC) (Steadman & Haglund, 2005; Cordner & Coupland, 2003). The EAAF and the FAFG were among the first international forensic anthropology groups that excavated mass graves in Argentina and Guatemala (Snow, 1984). The group PHR was formed in 1996 by an NGO based in Boston. The organization focuses on using medical and scientific methods, such as forensic anthropology, to investigate human rights abuses. The ICRC aids in a number of ways including strengthening international humanitarian law, protecting civilians, locating family

members, conducting forensic investigations and teaching forensic techniques (Cordner, & Coupland, 2003).

History of Forensic Anthropology in Human Rights Investigations

In the past, forensic anthropology techniques have been used to identify remains of U.S. soldiers from World War II, the Korean War and the Vietnam War. These investigations were limited, carried out by military and mortuary personnel who uncovered the graves, photographed the remains and reburied them (Steele, 2008). Proper techniques were not applied to systematic investigations of mass graves until the mid-80s in Argentina. During the period of military rule, 1974-1983, thousands of citizens were kidnapped, tortured, and murdered by the Argentinean military. They left likely over 9,000 missing individuals in their wake (EAAF, 2007). In 1984 the Argentinean government and the “Grandmothers of the Plaza de Mayo”, a human rights group of mothers and grandmothers, first sought out The American Association for the Advancement of Science to aid in the identification of the “disappeared”; thousands of individuals who were either killed or missing during the period of military rule (Buchli et al., 2001). The Association sent seven forensic scientists, among them the prominent forensic anthropologist Clyde Snow. Because previous exhumations were conducted by gravediggers and policemen, Snow compiled a number of Argentinean anthropologists to assist. This innovative approach to recovery was done alongside policemen, judges and relatives of the victims. Through Snow’s training the anthropologists formed the first group to apply forensic anthropology to human rights investigations, the EAAF (Snow, 1984). Subsequently, in the late 80s and early 90s more

forensic teams formed in Guatemala, the FAFG, and Chile to investigate mass graves (Haglund et al., 2001).

In 1995, PHR conducted an assessment of a mass grave that resulted from the 1994 Rwandan Genocide under the auspices of the International Criminal Tribunal for Rwanda (Haglund et al., 2001). The grave was located at Kibuye Catholic Church. In one specific event approximately 5,000 Rwandan Tutsi citizens gathered at the Kibuye Catholic Church. The church had been surrounded by police officers and armed Hutu civilians who attacked and killed the citizens over a period of days (Verwimp, 2004). These murders resulted in numerous mass burials as well as unburied surface remains. Forensic anthropologists and archaeologists from PHR collected surface remains and excavated the mass grave near the church. They conducted an analysis of age-at-death, sex, and ancestry estimation along with an inventory of possible traumas and associated artifacts. After all remains were collected the minimum number of individuals was estimated at 493 (Haglund et al., 2001). Because of security issues, this was the only grave excavated by forensic anthropologists in Rwanda (Steadman & Haglund, 2005). This is a common occurrence as political climates in areas recovering from human rights violations are often unstable. The UN and local governments provide as much security as possible, but often excavations must be postponed until safety can be established (Steadman & Haglund, 2005; Steel, 2008; Cordner & Coupland, 2003).

Protocol for Mass Grave Investigation

A mass grave has been broadly defined by the scientific community as, "...any location containing two or more associated bodies, indiscriminately or deliberately placed, of

victims who have died as a result of extra-judicial, summary or arbitrary executions, not including those individuals who have died as a result of armed confrontations or known major catastrophes” (Jessee & Skinner, 2005, p.56). There is no standard protocol for the investigation of mass graves. However, various methods differ between NGOs and countries and are established within the investigation’s needs. An NGO or local group will usually have Standard Operating Procedures (SOPs) for tasks such as site assessment, excavation, exhumation and autopsy procedures (Skinner et al., 2003). However, during any excavation the analysis of contextual relationships is of great importance. The relationship between two bodies, or a body and restraining device will reveal information about cause of, or events around the time of death. Bodies found in compromising positions, for example, dislocated cervical vertebrae resulting from a broken neck will not maintain that juxtaposed arrangement after they are transported to a laboratory. Only contextual observation will yield this evidence (Mundorff, 2012). Stratigraphic relationships can provide information about the sequence of the crime from the killing, to burial and post-burial disturbance (Steele, 2008). These are archaeological concepts that translate well to mass grave investigation. Other issues that investigators must commonly deal with are fragmentary and commingled remains.

II. Commingling

The positioning of the bodies is an important detail when determining the activities that led up to the creation of the grave. Bodies can be placed orderly in a supine arrangement, evenly spaced, and faced in the same direction. This indicates a burial created with respect. However, in cases of human rights abuse, bodies are more commonly found in

haphazard positions having been indiscriminately dumped into the grave or with evidence of execution such as blind folds and hand bindings (Komar & Buikstra, 2008). This indicates hasty disposal of remains and criminal activity. Beyond establishing forensic context, commingling poses a serious problem for identification when bodies have been disarticulated or have skeletonized.

The commingling of remains is due to both taphonomic processes such as bioturbation and animal scavenging, and human activity such as burning, intentional disarticulation, and reburial (Haglund & Sorg, 1997). Commingling can involve a mixture of human bone, animal bone, and non-organic elements. However, in the context of human rights violations commingled refers to a mixture of skeletal elements belonging to a number of people (Ubelaker, 2008). Commingling of human remains in a primary mass grave can happen naturally as bodies decompose and lose soft tissue that associates body parts and bones. This problem becomes more complex when one grave is added to another, when remains are intentionally damaged or when a grave is moved after a period of time (Jessee & Skinner, 2005; Haglund, 2001; Turner et al., 2008). Too often remains are never reassociated and end up being returned unidentified to the community they most likely belong to (Turner et al., 2008). Commingling issues can also be caused during exhumation process. This can happen if evidence bags are mislabeled or the location is not recorded. This is why proper archaeological techniques and documentation during the exhumation are imperative (Turner et al., 2008). Various reassociation techniques have been created to deal with commingling.

Current Reassociation Methods

Current reassociation methods include morphological techniques, mathematical and statistical models, X-ray, fluorescence, molecular analysis and chemical analysis. Morphological techniques consist of segregating based on age (such as epiphyseal closure) (Adams & Byrd, 2006; Adams & Konigsberg, 2004), establishing joint congruence between cervical vertebrae (Buikstra & Gordon, 1980), individualizing by the weight of long bones (Baker & Newman, 1957) and visual pair matching bilateral bones by robusticity, muscle markings, epiphyseal shape, bilateral expression, pathology and general symmetry (Adams & Konigsberg, 2004). Osteometric sorting is another morphological technique employed by measuring size and shape and creating a regression model based on the linear relationship between two bones (Byrd, 2003). Fluorescence techniques involve ultraviolet fluorescence in which remains are soaked in ultraviolet fluid and sorted under ultraviolet excitation according to differing color patterns (Eyman, 1965) and comparing the color variation of bone after exposed to short wave ultraviolet color variation (McKern, 1958). Chemical techniques include measuring trace element levels such as magnesium, zinc or sodium ratios (Fulton et al., 1986) and comparing isotopic strontium levels (Finnegan & Chauduri, 1990). A statistical method created by Snow and Folk (1970) determines the probability that a skeletal assemblage with no duplication may contain two individuals. Beyond these methods, DNA analysis can also be used to reassociate remains and make identifications.

DNA is an accepted form of identification when anthropological and odontological methods cannot be employed (Holland et.al. 1994). For example, it is effective in mass disasters when remains are highly fragmented (e.g. Twin Towers after 9/11) and

identification is the overall goal, or when there is no ante-mortem data to allow comparisons. One type of analysis uses nuclear DNA (Mundorff et al., 2008). In order to identify a person using nuclear DNA an existing sample must be available for comparison. This is commonly used to link a criminal to a homicide in forensic cases (NIJ, 2002). However, in the context of a mass grave, factors such as decomposition or burning of remains may prevent extraction of nuclear DNA and comparative samples are usually not available. Another form of DNA used for analysis is mtDNA (mitochondrial DNA). Mitochondrial DNA is passed down through the maternal lineage, so that each individual of such lineage shares the same mtDNA. There are thousands of copies of this type of DNA in our cells and it can be extracted from a very old or degraded source. DNA samples from victims are compared with DNA from possible family members. Mitochondrial DNA analyses are often used in mass grave scenarios (Komar & Buikstra, 2008). However, there are various limitations to DNA analysis. DNA extraction from bone is destructive and analyses may yield inconclusive results if, for example, the sample is contaminated, degraded or too small. Mitochondrial DNA successfully identifies family groups, but does not differentiate between closely related individuals like cousins or brothers. Also, false positives may occur when two unrelated individuals share the same mtDNA. Lastly, DNA comparisons have a long back log due to the high volume of requests and time it takes to complete an analysis. These are deterrents for using DNA to reassociate remains and make identifications in the context of human rights (Komar & Buikstra, 2008). Even with such a large suite of methods to choose from age, articulation, visual pair-matching, osteometric sorting, taphonomy and DNA analysis are the most commonly employed methods to reassociate commingled remains (Byrd, 2008).

III. Taphonomy

Forensic taphonomy allows one to reconstruct events that took place around the time of death by analyzing data in a depositional context (Ubelaker, 1997). A thorough understanding of taphonomy can help investigators determine peri and postmortem processes that contributed to commingling and therefore aid in reassociation. Much of the taphonomic research relies on the use of analogies and applying contemporary observations to make inferences about past occurrences. This is referred to as “actuality research” (Binford, 1977). This type of research is appropriate in a forensic context because the past and present conditions are generally the same; however, when comparing research with a crime scene one must make sure the two environmental contexts are similar. For example, a foundational actualistic study is that of Behrensmeyer (1978) who observed post-mortem skeletal changes on animals in the Amboseli Basin of southern Kenya. Animal carcasses of known ages ranging from fresh to 15 years of age were observed over a period of 2 years. Skeletal weathering stages were developed that can be applied to bones to obtain a general postmortem interval. More actualistic studies followed Behrensmeyer to obtain area specific weathering patterns and stages that could be applied to smaller creatures (Ross & Cunningham, 2011; Cunningham et al., 2011). Actualistic research relating to human burials is more complex. Parts of the taphonomic process that are important include environmental conditions, animal activity, and human activity. Patterns of animal chewing and gnawing on remains are distinguishable from ante or perimortem trauma. Animal scavenging can result in secondary deposition and is also recognizable. Environmental conditions contribute to the

degree of weathering and diagenesis of remains. Environmental conditions include soil type, sun exposure, fluvial transport and geochemical changes (Ubelaker, 1997). Insect activity also depends on environment as well as climate (Cunningham et al., 2011). Common in the context of human rights violations, human activity includes reburial, burning and other forms of intentional destruction. Within the post-mortem time period, these primary and secondary contexts modify both soft tissue and bone in different ways (Haglund & Sorg, 1997).

IV. Geographic Information Systems (GIS)

Geographic Information Systems (GIS) are computer technologies that create and store maps and analyze spatial relationships of structures or objects within maps. GIS can incorporate information about objects such as size or specific features into the analyses (Neubauer, 2004). GIS uses a national coordinate system that is compatible with various types of maps that use the same system. Of specific interest to archaeologists is a GIS program's ability to map stratigraphy as well as the objects within it in three dimensional space with three dimensional coordinates. This allows one to create profile maps displaying stratigraphy and its relationship to artifacts. The creation of a digital map also generates conclusive documentation of a site so it can be analyzed after it has been destroyed. Within archaeology, GIS has been used as a predictive model to locate sites across the landscape (Wescott & Brandon, 2004). This is particularly useful in cultural resource management and has been used to plan development projects that avoid archaeological sites (North Carolina Department of Transportation, 2012). It has been used to map individual sites to allow visual analysis of information after the excavation (Nigro et al., 2003). Within zooarchaeology it

has been used to establish minimum number of elements (MNE) and minimum number of individuals (MNI) by mapping and counting overlapping bone fragments (Marean et al., 2001). GIS has also been applied to criminal investigations. In this context it is used to examine the spatial dynamics of offenders or the interaction of the offender and the victim in time and space. To put it simply, investigators use GIS to map the geographic trends of crime (Chainey & Ratcliffe, 2005). Mapping crime data allows law enforcement to improve crime prevention and detection as well as understand criminal behavior.

GIS Programs

There are a number of GIS programs that can be used to analyze spatial data. Some are open source while others are proprietary software. These programs have similar functions but are often geared toward certain disciplines and types of data. GIS programs work with two types of data: raster and vector data. Raster data is represented by small cells or pixels that each holds a number. For example, each cell holds a categorical land cover value or continuous elevation value. Vector data is represented by points, lines and polygons that correspond to coordinates (GIS Dictionary). Some proprietary products include ArcGIS and IDRISI. IDRISI is a program directed toward environmental management and sustainable resource development that works mainly with raster data, while ArcGIS has broader applications and works with both raster and vector data (Chan, 2011). Open source software can be downloaded and used freely while proprietary software requires licensing that must be purchased. There are eight open source programs comparable to proprietary products. These include GRASS GIS, Quantum GIS, ILWIS/ILWIS Open, uDig, SAGA,

OpenJUMP, MapWindow GIS and gvSIG (Steiniger & Hunter, 2013). One of the more popular open source programs is GRASS (Geographic Resources Analysis Support System). This program works with 2D and 3D raster and vector data as well as voxel (volume) data and experiences continuous updates and bug repairs (Hall & Leahy, 2008).

GIS within Forensics

Most GIS analyses focus on large geographic areas in order to identify geographic trends and spatial relationships in society and the environment. Analysis of smaller areas, such as the room of a house, is less common but very useful in the context of a crime scene investigation (Little et al., 2000). Spatial analysis of crime scenes has been used to re-create suspect movement through the environment (Agosto et al., 2008). Three dimensional data collected at crime scenes has been used to create general crime scene maps using computer programs such as CAD Zone (Gardner & Bevel, 2009). These crime scene maps are typically not released to the public. However, a crime scene map was recently created by the author using total station points in ArcGIS (Figure 2.2). This map aided the police in documentation of the crime scene for future reference and court proceedings. Maps created with 3 dimensional total station data are very precise and are received well in a court room. Also, with the development of technology, re-creations with full scale computer generated features such as buildings or people, are being introduced in court. This sometimes has a negative impact because if the data sources and technological processes used to create it cannot be explained the evidence may be thrown out (Gardner & Bevel, 2009).

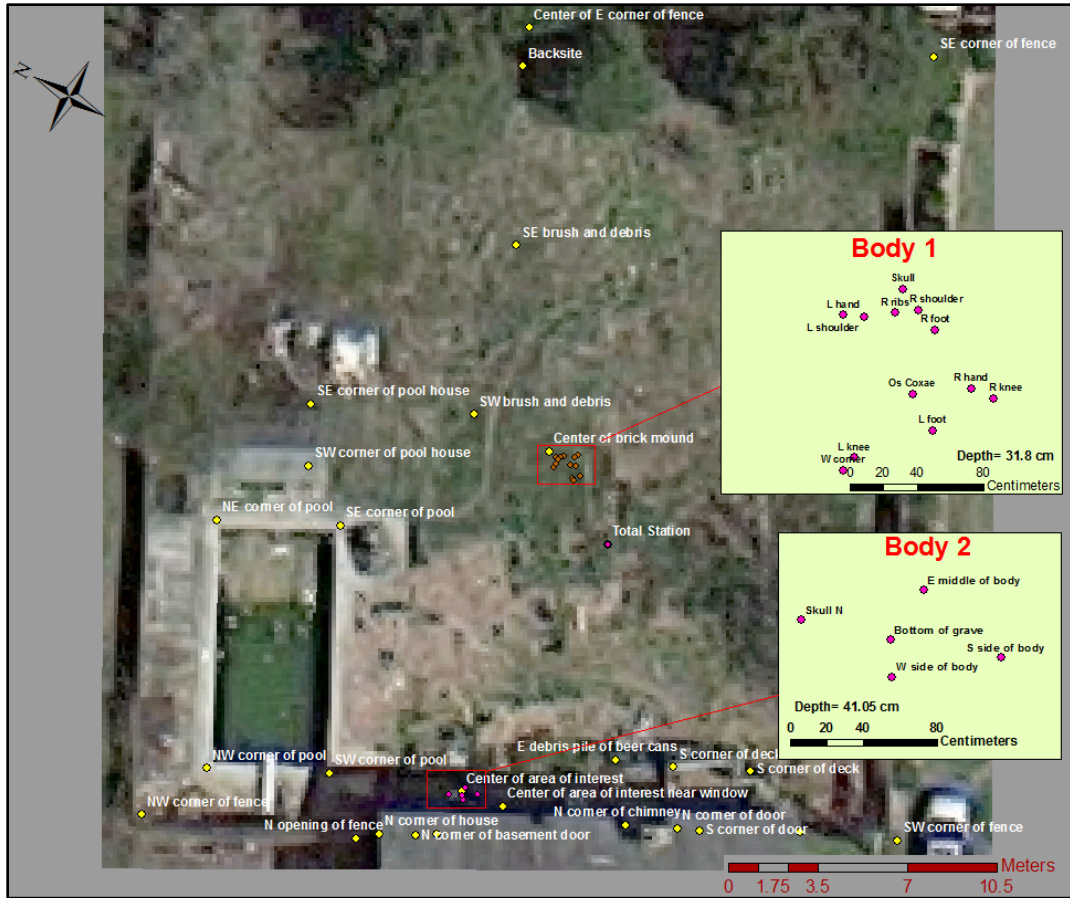


Figure 2.2 Crime Scene Map Created by the Author

V. Total Station Survey and Mapping

A total station is an electronic theodolite instrument integrated with an electronic distance meter (EDM). It is used to take precise coordinate, distance or angle measurements. Total stations can have either internal data storage and or an external data collector depending on the model. The machine may require a prism or be a prism-less model. It is most commonly used in surveying, but has also been applied in archaeology and crime scene

mapping (Neubauer, 2004; Gardner & Bevel, 2009; Nee et al., 1997). The total station records three dimensional coordinates with three internal devices: the EDM, the theodolite and the internal level. The EDM measures distance by sending multiple wavelengths of infrared carrier signals which are reflected by the prism or object being surveyed. A theodolite, or electronic transit, measures the angle of an object in the horizontal plane. An internal level measures the rise of an object in the vertical plane (Nee et al., 1997). While the total station collects the same data one would collect with a measuring tape, line level and grid paper, the value lies within speed and ease of taking measurements as well as what one can do with the data once uploaded onto a computer. Viewing the evidence in exact provenience using a GIS program will also allow the investigator to analyze the context or look at the relationships between items. One can also transform total station coordinates into a real world coordinate system using GPS. Photographs of a site or area can be integrated with total station data so that they are to scale, a process known as rectification. A vertical photo of the site must be taken. Control points can then be measured with the total station in the N, S, E and W corners of the site on objects visible in the photo. Using georeferencing tools, the photo can be scaled and aligned with the four control points and the rest of the coordinate data in a GIS (Bernatchez & Marean, 2011). Figure 2.2 shows a google earth image referenced to total station coordinates.

Machine Set-Up (Sokkia Operator's Manual, 2002)

Obtaining accurate data from a total station requires knowledge of appropriate set up and use (McPherron & Dibble, 2002). Before setting up the total station an appropriate

benchmark, north location and back site should be established. The benchmark is the location of the machine and the back site is a second location in case the machine must be moved to take measurements that can't be seen from the benchmark. These locations should be permanently marked with re-bar or nail so the station can be taken down and set up again in the same location. The machine should be set up over the benchmark, leveled and turned on. Next, measurements of the machine and prism height are taken and input into the machine. The machine coordinates are set to 000, which is the location of the total station. North is then set by sighting in the fixed point chosen for North and 0-setting the machine. The back site is then sighted, measured and input as the back site. The operator is then ready to take measurements (Operator's Manual, 2002). A depiction of taking measurements is shown in Figure 2.3. These steps are very important if the operator wants to set up the machine another day and obtain comparable measurements. As one can imagine there can be significant error with machine set up and use.



Figure 2.3: Using the Total Station

Associated Error

Accuracy and precision varies by device, set up and use. Precision refers to the reproducibility of the measurement and accuracy refers to how close the measurement is to the objects actual location. The total station typically has an error of only 5 mm when used properly (McPherron, 2005). Error can be introduced into the measurements in various ways. If the prism is not held level, for example, swaying left to right or front to back, the North and East coordinate will be slightly off. Error can result if the beam is not directly focused on the prism. Care must be taken to center the view finder on the total station to center on the prism (Sládek et al., 2012). If there is any error when taking the measurement of the station or prism height the z coordinate (elevation) will suffer. The total station should be set up close to the objects of interest if possible, because measurement error increases with distance (Sládek et al., 2012). Sometimes the machine must be taken down and set up again numerous times to complete a lengthy project. The station must be placed in the exact location during re-set up and the north must be re-set to the exact same horizontal location. If these locations differ slightly there will be error in the subsequent measurements (McPherron & Dibble, 2002). One way to deal with this is to create fixed points with a material like re-bar and draw a small point in the center with permanent marker during the first set up. This will allow the operator to get as close as possible to the same initial location.

Mapping crime scenes and mass graves

The application of traditional research-oriented excavation techniques and methods to modern forensic sites and crime scenes is referred to as forensic archaeology (Tersigni-Tarrant & Shirley, 2013). The systematic excavation of a site is intrusive and will almost certainly cause the destruction of the crime scene. Investigators may have to recreate the crime scene accurately years later. Because of this, it is important to thoroughly document a crime scene as evidence is removed, a concept known as controlled deconstruction.

Documentation of a crime scene refers to the collection of data through written field notes, photography and hand drawn maps. Provenience is the three dimensional location of an object. An item's provenience is mapped by placing a kind of grid over the crime scene and measuring its location from the site boundaries with a tape measure (Tersigni-Tarrant & Shirley, 2013). The z measurement, or depth of an object, is traditionally collected with a string, line level and tape measure. These data is recorded with a pencil and graph paper to make a map. Photogrammetry is often used to make precise measurements using photographs. This means a scale, such as a tape measure, is used in the photo to re-create the size of unmeasured objects (Gardner & Bevel, 2009). More recently, the quick and precise documentation capabilities of a total station have been utilized at archaeological sites and crime scenes to measure provenience (Neubauer, 2004; Gardner & Bevel, 2009).

Some concepts that forensic archaeologists use to analyze crime scenes include the law of superimposition and the law of association. The law of superimposition states that the oldest layer is on the bottom, while the law of association states that proximity of two items and the integrity of the deposit they are found in determines the significance of their

relationship (Skinner, 1987). This translates to sequence of deposition and significance of context. Within crime scene investigations the importance of contextual relationships cannot be exaggerated. “Context often matters more than content- a grave often says more about its occupant, and the cause of his or her death, than do the occupant’s bones themselves” (Snow, 1995 pg. 17). Detailed recording processes and the collection of contextual data are often skipped over in order to save time or reach the short term goal of repatriation to families. However, this actually results in drawn out reassociation and identification processes (Cabo, Dirkmaat, Adovasio & Rozas, 2012). Comprehensive recordation of the context, such as spatial distribution of the remains will enhance the reassociation and identification process.

VI. Studies Incorporating GIS into the Analysis of Human Remains

Spatial analysis using GIS has recently been applied to investigate the deposition of human remains. In 2006, a study assessed the correlation between dispersed human remains on the ground surface and the postmortem interval (Manhein et al., 2006). The study used 36 cases of mapped and recovered human remains in Louisiana. A Cartesian coordinate system was created in ArcView from crime scene maps in which the original dump site was the $x=0$, $y=0$. Their results indicated that as more time passed remains did become more geographically dispersed but not significantly. A second study, by the same authors in 2007, investigated the use of GPS for mapping dispersed surface scatter of human remains (Listi et al., 2007). A GeoExplorer® 3 Data Collection System, which is capable of sub meter accuracy after differential correction, was used. They compared the GPS measurements to traditional field methods using a tape measure and datum. Their results found that the GPS

measurements had an error of around 1.5 ft and therefore cannot be used for mapping heavily clustered surface scatter. However, mapping the general location of a site or crime scene can be quite useful.

The mapping of mass graves using survey equipment and GIS has been employed and proven quite useful. Spatial analysis has also been conducted in mass grave settings. Laser survey equipment, such as total stations, can be used to map the position of a body or the location of evidence with three dimensional coordinates. These data can then be uploaded into software to recreate the scene for further analysis. Such precise three dimensional coordinates could also be used to perform spatial analysis of commingled remains in an attempt to reassociate them. The laws of spatial analysis dictate that objects that are close to each other in space are most likely associated (Tobler, 1970). While it is more commonly the approach to reassociate commingled remains at autopsy than in the field, recent cases have involved analyzing the contextual provenience of body parts in the grave in order to reassociate individuals. Investigation of this concept was undertaken by Tuller and co-workers (2008). Their study served to inform practitioners of the potential of precise mapping and spatial analysis. The study was carried out ad hoc on a secondary mass grave in Bosnia after reassociations and identifications had already been made. Microsoft Access was used as the GIS database, which can complete the analysis but cannot create a map. They used 15 survey points to record a body and focused on reassociating whole body parts, ignoring individual or fractured bones. Further controlled research conducted on a primary deposition of fully skeletonized remains will reveal the true potential of this technique and allow for a detailed replicable protocol to be created.

CHAPTER 3: Materials and Methods

I. Using Pigs as a Proxy for Humans

A mass grave commingling was recreated using domestic pigs (*Sus scrofa*). Pigs have proven to be an acceptable analog for human subjects. They are known to share similar nutritional and physiological patterns with humans. Pigs have similar fat distribution, body hair, internal anatomy and chest cavity size (Catts, 1992; Byrd & Castner, 2001). Because they are omnivores their metabolism rates and gut bacteria are comparable (Patterson et al., 2008). In terms of bone mineral density, pigs are the most similar animal to humans with dogs as a close second (Aerssens et al., 1998). Because of these parallels, they are used in various types of biological studies concerning human nutrition, pathology, dentistry, and decomposition (Nielsen et al., 2014; Weaver et al., 1962; Schoenly, 2006). While pigs are domesticated for the purpose of food, they are some of the most readily available research subjects. They reproduce and grow at a fast rate that is only increasing with developments in feed and housing improvements (Aumaitre et al., 1982).

Ten pigs were used for this project ranging in development from infant to adult both male and female. This would represent the demographic found in a mass grave related to genocide, a situation in which individuals of a specific ethnic group are harmed indiscriminate of age and sex (OSAPG, 2014). Notable examples of mass graves resulting from genocide include those recovered in Rwanda and Srebrenica, Bosnia (Neuffer, 1999; Stover & Peress, 1998; Caplan, 2007; Maxwell & Ross, 2011). Pig sizes ranged from 4-150 lb. Specifically, two fetal, two 50 lb, two 70 lb, two 90 lb, and two pigs between 100-150 lb

were used. This aided in the projects control, which included distinguishing pigs based on bone size differences.

The pigs were obtained from the North Carolina State University (NCSU) swine farm by committee member Dr. Wes Watson according to NCSU REG 10.10.01, the Animal Care and Use Procedures. This regulation requires an approved Application for Vertebrate Animal Use and communication with the Institutional Animal Care and Use Committee. Eight of the pigs were humanly euthanized by captive bolt pistol at the swine farm. The fetal pigs were not euthanized as they died of natural causes during birth. The pigs were euthanized a few hours prior to the study. Swine farm employees transported the pigs to the Lake Wheeler Field Site and placed them in the grave.

II. The Research Field Site

The study was conducted on land owned by NCSU in the Lake Wheeler area. The grave site was located behind a cornfield just in front of a heavily wooded area. The soil consisted of clay-loam according to a Munsell color chart, which categorizes soil types by color and texture (Munsell & Color, 2000). The grave site consisted of an open pit that measured 10'24'' (312 cm) by 8'53'' (260 cm) in length and width and 6' 4'' (195 cm) in depth. The pit was excavated by the NCSU Lake Wheeler field crew in 2012 when it was initially used for another decomposition study (Honeycutt, 2012). To allow water drainage during rain storms the field crew installed a pipe running from the bottom of the grave underground to an area of lower elevation. A wire screen was placed in front of the drainage

hole to prevent clogging or loss of bones. The pit was cleaned out and reutilized for the present study (Figure 3.1).



Figure 3.1: The Lake Wheeler Field Site Being Renovated

On January, 17, 2014 the pigs were placed in the grave. The pigs were arranged close together so that limbs were overlapping to encourage commingling. Care was taken to place pigs of the same size on opposite sides of the grave to aid in overall control. A total station was used to record the initial position of the pigs. The total station was placed 1 meter away from the corner of the grave. A benchmark, back site, and second fixed point were created so that the same coordinate system could be used during the excavation. Points were taken on the head, thorax, and backside of each pig to capture orientation. The points were associated with individual pigs according to their size. For example, measurement 1 was the first 150 lb pig's head and so on (Figure 3.2). Three pieces of re-bar and a nail were placed in the grave

to serve as control points from which to observe movement. Points were also taken on these nails.



Figure 3.2: Total Station Points Referenced to a Vertical Photograph

Once the pigs were placed in the grave and recorded with the total station a metal cage was constructed around the grave to keep out animal scavengers. Materials consisted of 1 inch metal piping, 1 inch elbow pieces, 1 inch PVC pipe and 1 inch mesh chicken wire.

The metal piping was placed in the ground around the four corners and on the sides of the grave. Metal elbow pieces were used to connect piping in order to create a wire frame. Chicken wire was wrapped around the frame and secured with plastic cable ties. An opening to the grave was created on the front side of the cage. The opening consisted of a flap of chicken wire connected to the cage with electrical wire. This allowed for internal maintenance when needed (Figure 3.3). A scale made of 4 meter sticks sitting on top of cinder blocks was placed in the corner of the grave. This was included so all photographs taken of the grave would have a scale.



Figure 3.3: Cage Built to Protect the Remains from Scavengers

III. Sokkia SET 10 Total Station: Protocol for Set Up

Before setting up the total station, an appropriate benchmark, north location and back site were established. The benchmark is the location of the machine and the back site is a second location in case the machine must be moved to take measurements that cannot be seen from the benchmark. These locations were permanently marked with re-bar so the station could be taken down and set up again in the same location. The machine was set up over the benchmark, leveled and turned on. Next, height measurements of the machine and prism were taken and put into the machine. The total station accounts for these measurements when calculating the location of the object being measured. The machine coordinates were set to $N=0$, $E=0$, and $Z=0$ which means everything will be measured in relation to the total station. North was then set by sighting in the fixed point chosen for North and 0-setting the machine. The back site was sighted, measured and input as the back site. The machine was then ready to take points. This protocol was followed for every set up.

IV. Time Lapse Photography and Aerial Photographs

Part of the control for this study is the measurement of movement from vertical photographs using time lapse photography. A Cannon Rebel XS, which is a digital point and shoot camera, was used. Time lapse functions were made capable with a time-lapse intervalometer, which is a remote control timer. This device was plugged into the camera and programmed to take a photograph every hour. The camera took hourly photographs, only during the day due to battery life. Batteries in the camera were changed every day. In

order to leave the camera outside all day it needed protection. A weather proof camera container was created with an ammo box. A small camera lens sized hole was cut in the bottom of the ammo box. A circular piece of plexi-glass was placed in the hole and sealed with glue. The camera, with the lens placed over the glass, and the remote control were secured in the ammo box protecting the devices from the weather. To get detailed vertical photographs of the grave, the camera needed to be placed directly over the grave at a close distance. There also needed to be a way to remove the camera every day to change the battery and put it back in the same exact location. A sliding mechanism was employed that allowed daily removal. A metal rack was constructed over of the grave and inside the cage that fit the size of the ammo box. Metal fixings were placed on the rack that stopped the camera in the same place directly over the grave after every battery change. A piece of PVC pipe with a nail drilled into the end served as a hook to retrieve the camera from the center of the grave. The chicken wire in the area where the camera was removed was fastened with electrical wire that could be removed, similar to the grave opening (Figure 3.4). The photographic process was facilitated by Forensic Photographer Gary Knight.



Figure 3.4: Camera Set Up. Left- Camera battery being changed. Right- Camera being slid back into the original location on the rack.

V. Excavation

The pigs were allowed to decompose and commingle over the course of 3 months. On October 16 the cage was removed, but the camera was left in place in order to take pictures during the excavation. The grave was gridded into 6 meter x 6 meter units using white string and chaining pins. This was done to create organization during the mapping process and to create separate areas for more detailed referencing. The excavation began on October 17. The back site and second fixed point were measured and compared to the initial points to detect error. This was done for every set up to assess the overall error in the total station measurements. If error was high (over 1 cm), the total station was checked and reset-up. On average, the back site was no more than 2 mm off and the second fixed point was no more than 5 mm off. Measurement information is shown in Tables 3.1 and 3.2.

Table 3.1: Back Site Coordinates (in meters)

Back Site Coordinates			
Date	N	E	Z
Original	16.962	0.006	0.87
17-Oct	16.966	0.005	0.874
18-Oct	16.966	0.006	0.875
21-Oct	16.952	-0.001	0.872
24-Oct	16.960	0.000	0.871
26-Oct	16.968	0.006	0.871
1-Nov	16.961	0.006	0.871
3-Nov	16.952	0.000	0.871
15-Nov	16.967	0.000	0.869
16-Nov	16.964	0.006	0.871
14-Dec	16.962	0.006	0.870
20-Dec	16.967	0.006	0.871
Average	16.962	0.0038	0.871

Table 3.2: 2nd Fixed Point Coordinates (in meters)

2nd Fixed Point Coordinates			
Date	N	E	Z
Original	1.281	9.762	-0.341
17-Oct	1.280	9.762	-0.340
18-Oct	1.284	9.765	-0.341
24-Oct	1.285	9.755	-0.338
26-Oct	1.287	9.770	-0.337
1-Nov	1.288	9.766	-0.340
3-Nov	1.288	9.765	-0.388
15-Nov	1.295	9.771	-0.334
16-Nov	1.286	9.765	-0.338
14-Dec	1.287	9.759	-0.340
20-Dec	1.284	9.772	-0.338
Average	1.2864	9.765	-0.3434

Each unit was measured at the corners with the total station prior to excavation in order to create control points for Georeferencing. Units were identified as numbers 1-6. Unit 1, which was closest to the grave entrance, was mapped first. Units are shown in Figure 3.5. Four letter codes were used to identify bones. These codes correspond to bone type and the location on the bone. Areas of articulation were mapped so that disarticulated bones could be reassociated with the closest missing elements. Both proximal and distal ends of long bones were mapped so that orientation would be accounted for in the reassociation process. For example, a proximal ulna should be reassociated with the closest distal humerus; this is differentiated from a proximal humerus. Codes did not include sides or differentiation between carpals and tarsals, vertebrae types, rib types, and front and hind metapodials (equivalent to human metacarpals) and phalanges. This was done in an effort to save time. Bone side and specific type were determined post-excavation. Codes are presented in Table 3.3. Once a bone was mapped it was placed in a paper bag with the total station id number, code and coordinates written on it. In order to reduce the number of bags used, different types of bones were placed in the same bag. This allowed every bone to stay associated with its total station ID and provenience. This information was also recorded in a coordinate log to create a backup set of data. To do this, the coordinates were read aloud by the operator after every measurement. This also lets the operator know every measurement was being recorded by the total station. A long prism was used due to the depth of the pit. In order to hold the long prism steady one person must hold it on the bone while another keeps it level (Figure 3.6). Five people were needed for the process to run efficiently: one total station operator, two prism operators, one evidence bagger and one coordinate log recorder. This

process was used on the first and second day of the excavation. Subsequently it was found that a smaller prism was still visible to the total station and could be held by one person (Figure 3.7). Evidence bags from each day were sealed in a cardboard box with the date and stored in cool dry location. Between work days the grave was covered with chicken wire that was secured to the ground with metal stakes.

Table 3.3: Bone Codes

BASI - cranium, taken on the middle of the basilar area	PFEM - proximal femur, taken at proximal articular surface
OCCL - cranium, taken on the right occipital condyle	DFEM - distal femur, taken at distal articular surface
OCCL - cranium, taken on the left occipital condyle	PATL - patella, taken at middle of exposed bone
VERT - vertebrae, taken at middle of exposed bone	PTIB - proximal tibia, taken at proximal articular surface
SCAP - scapula, taken at middle of glenoid fossa	DTIB - distal tibia, taken at distal articular surface
RIBH - rib, point taken at costal facet, or head	PFIB - proximal fibula, taken at proximal articular surface
RIBS - rib, point taken and sternal end	DFIB - distal fibula, taken at distal articular surface
PHUM - proximal humerus, taken at middle of proximal articular surface	TALU - talus, taken at middle of exposed bone
DHUM - distal humerus, taken at middle of distal articular humerus	CALC - calcaneus, taken as close to articular surface as possible
PRAD - proximal radius, taken at middle of proximal articular surface	OCX1 - os coxa, taken at middle of sacro-iliac joint
DRAD - distal radius, taken at middle of distal articular surface	OCX2 - os coxa, taken at mid acetabulum
PULN - proximal ulna, taken at proximal articular surface	OCX3 - os coxa, taken at middle of pubic symphysis
DULN - distal ulna, taken at distal articular surface	OCX4 - os coxa, taken at middle of unfused surface
CARP - for both carpals and tarsals, taken and middle of exposed bone	STER - sternum, taken from middle of exposed bone

Table 3.3 continued

DMET - Distal Metapodial, taken at distal articular surface	MANL - mandible, taken on left mandibular condyle
PMET - Proximal Metapodial, taken at proximal articular surface	MANR - mandible, taken on right mandibular condyle
PHAL - Phalanx, taken from center of exposed bone	EPIP - Epiphyses, taken in the middle of exposed bone



Figure 3.5: The Grave Mapped in 6 Meter x Meter Units



Figure 3.6: The Long Prism must be Operated by Two People



Figure 3.7: The Smaller Prism can be Operated by One Person

Because the pigs were juveniles, bones consisted of unfused elements. Vertebrae were often in two or three pieces and long bone epiphyses were unfused. In the north half of the grave every bone, epiphysis and unfused element was recorded. In the south half only full bones and essential portions of unfused elements were mapped. For example, only the vertebral arcs were mapped, while the bodies were omitted. This was done in order to compare the time it would take to map all elements versus just the essential elements. The two strategies can also be considered the difference between highly fragmented assemblages versus un-fragmented assemblages containing adults with fully fused elements. Elements that were omitted were not disturbed. Long wooden planks were set on top of concrete blocks over the grave to allow the essential elements to be mapped without disturbing anything else. This was done so that if time permitted, the non-essential elements could be mapped in the end. It should also be noted that some fetal bones were not found. These bones moved a great deal within the grave and were too small to track through time lapse photography. The small bones were either covered with mud or washed through the drain during storms.

The excavation took a total of 2 weeks to complete. The first half of the excavation was completed with 4-5 people and the second half was completed with 2 people. While four is the ideal number of people, two is the minimum that can be used and it significantly slows down the process. The excavation was completed on 12/20/2014.

VI. Reassociation using GIS

Near 3D Analysis

ArcMap 10.2, a program in the ArcGIS suite, was used to make reassociations based on spatial relationships. Data were transferred from the total station to the computer as a text file using Sokkia Link, a program specific to Sokkia total stations. The text file was then converted to an Excel work sheet that is compatible with ArcGIS. Side, measurement and age information was then collected from the bones and added to the Excel sheet in separate columns. These data were loaded into ArcMap. A tool called Near 3D was used to complete the spatial analysis. This tool calculates the three dimensional distances from one set of data to the closest feature in another set of data based on xyz coordinates. For example, a group of left distal femora was compared with a group of left proximal tibiae. In order to use Near 3D, the data were split into separate feature classes representing left and right and proximal and distal portions of bones. The bones included in the analysis were scapulae, humeri, radii, ulnae, ilia, femora, tibiae, fibulae, tali and calcanei as they could be easily identified and sided. The closest missing elements for each group were found using Near 3D. Results were exported to Excel work sheets where they were checked for accuracy using the control methods. If the first closest match was incorrect, the next closest element was searched until the correct match was found. This was done by separating the incorrectly reassociated bone into its own group in ArcMap and comparing it to the entire group of closest missing elements so a distance was calculated for every bone. Small bones such as carpals, metapodials and phalanges could not be sided with confidence. However, associated clusters were identified using spatial statistics.

Hot Spot Analysis

Hot Spot Analysis [®], another tool in ArcGIS, was used to identify associated clusters of bones. This analysis calculates the Getis-Ord (GI*) statistic for every feature in the dataset. This statistic measures the degree of clustering and identifies high or low (hot or cold) levels of clustering in cells (Ord & Getis, 1995). In order to do this, points were converted to polygons by spatially joining a grid with the data points. The cell size chosen for the grid was .05 m as it captured spatial patterns the best. After the spatial join, each grid cell becomes a polygon containing a given number of points where each point is a bone. Z-scores and *p*-values are calculated for each cell, which determine hot and cold areas. Each cell's point count is compared with the point count in its neighboring cell. The sum for a cell and its neighbors (local sum) are compared to the sum of all the other cells in the grid. A high *z-score* results when the local sum is much higher than the expected sum indicating a hot spot. A spot can be hot or cold at a 90%, 95% or 99% confidence level which is indicated by the *p-values*. The inputs for this tool include the conceptualization of spatial relationships parameter, distance method and the fixed distance band value. "Fixed Distance Band", which is recommended for point data, was used for the conceptualization of spatial parameters. This means a distance band that determines which cells will influence other cells must be set. The distance method was set to "Euclidean Distance"; a straight line between two points. The value used for the distance band, when working with phalanges, was 0.119 m. This value is three times the standard deviation of the average distance between phalanges that was computed with Near 3D using phalanges as both the input and near feature. Anything further away was considered a spatial outlier. Distance bands of 0.108 m

for carpals, 0.207 m for vertebrae, 0.103 m for ribs and 0.102 m for metapodials were used. Ribs and metapodials are composed of two points: the head and sternal end of the rib; the proximal and distal ends of the metapodial. Only one point was chosen to represent each group. The rib head was chosen because it is articulated to a vertebra and likely to have undergone less movement than the sternal end that is only attached to cartilage. The proximal portion of the metapodial was chosen because this portion was initially closer to its original owner than the distal end.

VII. Methods for Control

Osteometric Sorting

Osteometric sorting is an accepted, commonly used method for sorting commingled remains in a forensic setting (Byrd & Adams, 2003). This method relies on size and shape differences between individuals that allow bones to be segregated. Osteometric sorting is most appropriate when there are various body sizes in the sample as is the case in this project. One would start with two bones, asking to examine if they are from the same individual. Regression is used to quantify the linear relationship between individual bones from a reference sample. Regression formulas are created to predict the measurement of the dependent variable. This value and other regression parameters are used to derive a *t*-value. *P*-values are then calculated using a two tailed *t*-distribution. A 90% prediction interval, alpha of 0.1, is used for sorting. This is suggested by Byrd and Adams (2003) as it offers the most acceptable results.

A reference sample is needed to create regression formulas. Such samples exist for human remains (i.e. the Forensic Databank). However, for this project a reference sample of pig measurements was created, which ranged from fetal to adult and came from three sources. One from NCSU, one from the North Carolina Museum of Sciences and 22 from the Smithsonian Institution were used. Many of these were partial skeletons and no skulls were measured. Therefore, only certain bones can be controlled for using this method. Beyond that, this method requires that the bones being sorted are correctly identified so they can be compared with the known sample. For this project, crania, vertebrae, phalanges, metapodials, ribs, carpals and tarsals were not included. While it is possible with human remains, it is difficult to distinguish between frontal and hind phalanges and metapodials in pigs. It is also difficult to side them. These bones look very similar in the pig due to quadrupedal locomotion (Hillson, 1999). Of the tarsals only the talus and calcaneus were used as they are easily identifiable.

Byrd and Adams (2003) found that taking both length and breadth measurements of a bone captured more information. Both length and breadth measurements were taken for each element. Bones were measured according to standards for animal bones outlined by Driesch (1976). Measurement tools included an osteometric board and sliding and spreading calipers. The measurements for each element were transformed into a single variable by adding them together and taking the natural logarithm. This captured both shape and size and made the values easier to work with. This was done for both the reference sample and the unknown elements. Statistical analysis was completed in SAS 9.4. The SAS proc reg procedure was

used (Freud & Littell, 2000). Regression formulas were created for pairs of each type of bone; for a total of 8 formulas.

Calculation of t and p -values from the regression parameters were done in Excel. T -values were derived using a formula modified by Byrd (2008):

$$t = |\hat{y} - y_i| / [(S.E.) \times \sqrt{1 + (1/N) + (x_i - \bar{x})^2 / (N \times S_x^2)}].$$

In this equation \hat{y} is the predicted value from the regression model, y_i is the dependent variable, S.E. is the standard error of the regression model, N is the sample size used to calculate of the regression model, x_i is the independent variable, \bar{x} is the reference sample mean of the independent variable and S_x is the reference sample standard deviation of the independent variable. P -values were calculated in Excel using the two-tailed Student's t -distribution. Every possible match was assessed and compared to the spatial analysis results. Bones were segregated when the p -value was below 0.1. However, a p -value above 0.1 does not mean the two bones belong together. This only indicates that there is above a 10% probability that the variation between the two bones resulted from chance.

Visual Pair Matching

Visual pair matching is a method in which bilateral bones are compared based on robusticity, muscle markings, epiphyseal shape, bilateral expression, pathology and general symmetry (Adams & Koningsberg, 2004). This was used to confirm the associations made using Near 3D ® that were also controlled with osteometric sorting. All paired elements were visually matched using this method. Adams and Koningsberg (2004) indicate it is

feasible to sort between elements when there is a small group of individuals that vary significantly in size, which is the case in the current project. Associations were made between elements by seriating the paired elements by size and then grouping them by size, taphonomy and morphology. One pig was covered in clay due to its placement in the grave. Another pig had significant periosteal reaction on most bones (See Figure 3.8). Another factor allowing sorting between elements was the original placement of pigs in the grave. Pigs of similar size were placed at opposite sides of the grave to avoid the elements of similar size from different specimens to be placed next to each other. Therefore it is highly unlikely for elements of similar size to be placed next each other. When there was a question of segregation based on visual matching the position of the bone in the grave was referenced. An example of this is presented in Figure 3.9.



Figure 3.8: Visual Matching Based on Morphological Similarities. Bilateral periosteal reactions are shown on the left and taphonomic similarities, clay staining, are shown on the right.

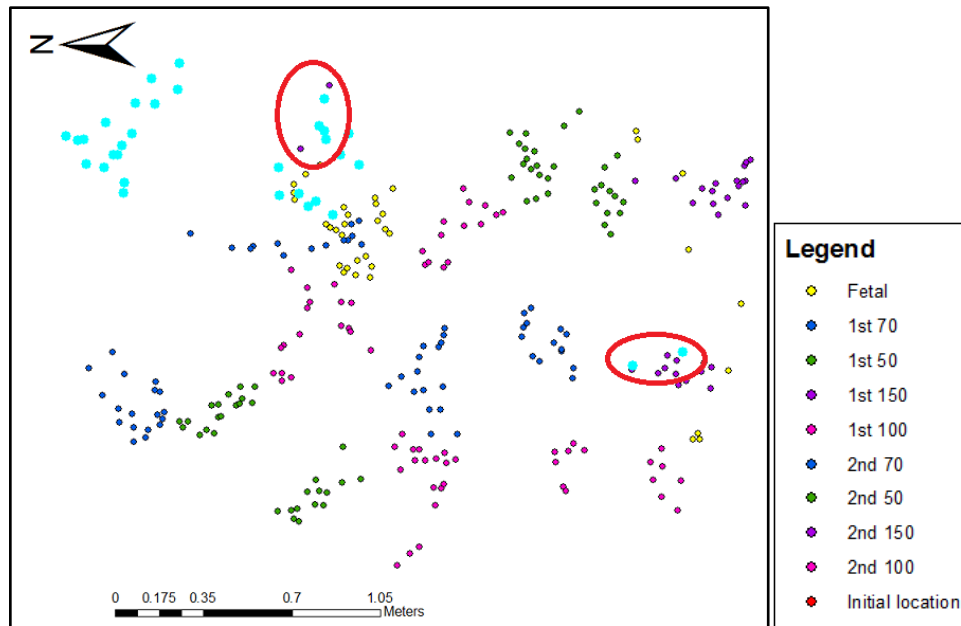


Figure 3.9: The Position of Bones in the Grave. The first 150 1b pig is highlighted in the top left corner. The points circled in red on the right represent scapulae selected for the first 150 based on visual pair-matching. It is more likely that the two scapulae circled in red on the left are associated with the highlighted pig.

Time Lapse Photography

Time lapse photography was used to track the location and movement over time of all bones large enough to be visible in the picture. A time lapse video was created from the hourly photographs taken every day. Visual tracking worked well for all bones except phalanges, carpals and metapodials. When osteometric sorting and visual pair matching did not agree the time lapse footage was referenced to assess the movement and final location of specific bones. Ribs, vertebrae, crania and mandibles were segregated by referencing the video and comparing the final photograph with the total station points. The time lapse video can be found online ([Pig Time Lapse](#)).

CHAPTER 4: Results

I. Results for Reassociation using GIS

Near 3D Analysis

Elements were correctly reassociated with the 1st closest match in 136 out of 148 cases (91.89%) using Near 3D. The 2nd closest element was correct in 11 cases (7.43%) and the 5th closest match was correct in one case (.67%). Of the 12 incorrect reassociations 8 (66.7%) were due to a mismatch between adult and fetal bone. The remains of the fetal pigs moved the most out of all of the subjects most likely due to their small size and light weight. The fetal pigs also decomposed quicker than juvenile pigs, which is consistent with taphonomy literature showing that size is a factor in decomposition (Hale & Ross, 2015). Bones tended to move toward the SE corner of the grave. This is due to a slight drop in gradient in the SE corner to facilitate drainage of rain water. Fetal and other smaller bones such as phalanges shifted toward the SE corner during storms when the grave filled with water. On average the closest missing element was 10.82 cm away. The closest matching pair was 1.53 cm away from each other. The most distant matching pair was 108.1 cm away from each other. This was a left fetal humerus and scapula. Again, this was due to the significant movement of fetal bones in the grave. Maps of the grave in which elements are individuated are presented in Figures 4.1 and 4.2. Figure 4.1 includes only the points, while Figure 4.2 includes the points and a referenced photo. The initial locations of the pigs are included in both maps to visualize the overall movement of elements. The direction of movement toward the SE corner of the grave can also be seen.

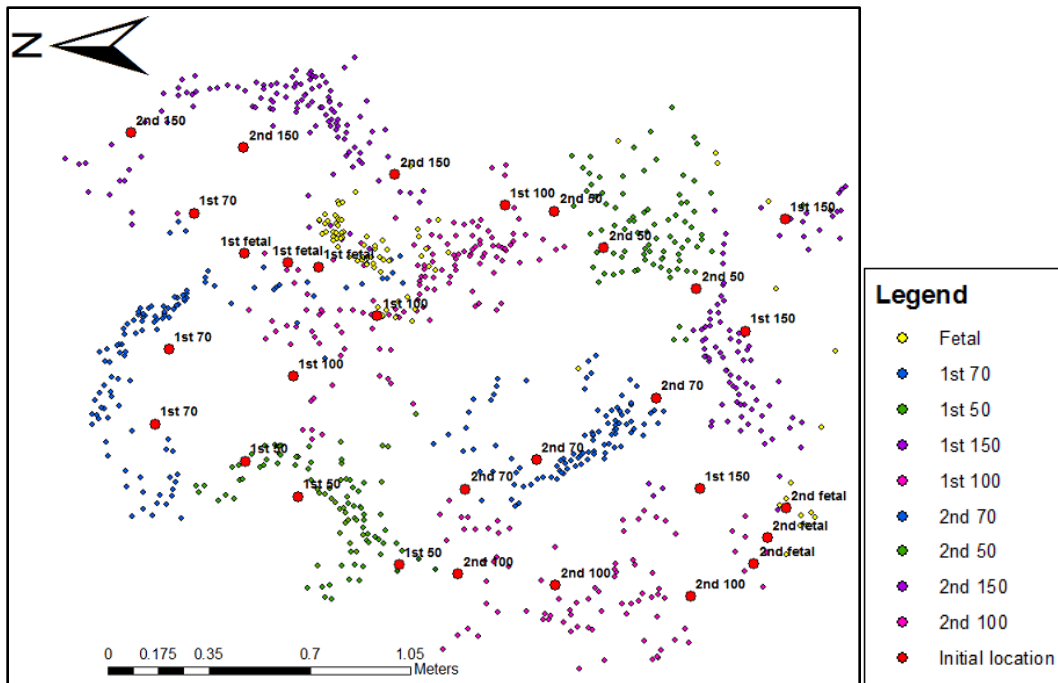


Figure 4.1: Individuated Skeletal Elements



Figure 4.2: Individuated Skeletal Elements Referenced to a Photo

Results for the reassociation of left humeri and radii are presented in Table 4.1. The first column titled “Number” shows the number assigned to the bone in ArcMap. The column titled “LN” is the natural logarithm of the summed measurements of the dependent variable; in this case that would be the humerus. The column titled “Xi” is the natural logarithm of the summed measurements of the independent variable; in this case that would be the radius. The column titled “Predicted” contains a formula from the regression model of radius on humerus. The values in this column are the predicted values from the formula. The column titled “Formula 1” contains the first part of Byrd’s *t*-value formula; =ABS (Predicted - LN). The column titled “Formula 2” contains the second part of the formula; =.10275*SQRT(1+(1/37)+(Xi-5.0176245)^2/(37*0.469441^2)) . The column titled “T-value” is Formula 1/Formula 2. The column titled “P-value” contains =T.DIST.2T (*t*-value, 36) with 36 degrees of freedom. This is the two-tailed *t*-distribution. The columns titled “642”, “826”, “880” and so on are the numbers for each radius tested with each humerus. Each match was tested by imputing the ln of each radius in the “Xi” column and copying the resulting *p*-values to the appropriate radius column. *P*-values lower than 0.1 indicate that the bones do not match. Cells highlighted in yellow indicate a correct match based on proximity. Cells highlighted in red indicate an incorrect match based on proximity. The cells highlighted in light blue indicate the true match if a match was incorrect. Results for the rest of the individual reassociations are presented in Appendix I. Overall results are presented in Table 4.2.

Table 4.1: Results for the Spatial Reassociation of Left Humeri and Radii

Right Humerus and Right Radius																				
Number	LN	Age	Xi	Predicted	Formula 1	Formula 2	T-Value	P-Value	Rad 642	Rad 826	Rad 880	Rad 1026	Rad 1255	Rad 1457	Rad 1526	Rad 1681	Rad 1895	Distance	Match	OS
Hum 377	5.0575		4.80648	5.092917	0.0354167	0.1044061	0.339221	0.7364	0.0263	0.5280	0.0000	0.0299	0.8239	0.4742	0.0620	0.0102	0.7364	0.3344	1st	6
Hum 627	5.2807		4.80648	5.092917	0.1877833	0.1044061	1.798586	0.0805	0.8628	0.1481	0.0000	0.8999	0.0860	0.1652	0.8298	0.5727	0.0805	0.2211	1st	4
Hum 655	4.1667	Fetal	4.80648	5.092917	0.9262467	0.1044061	8.871579	0.0000	0.0000	0.0000	0.9718	0.0000	0.0000	0.0000	0.0000	0.0000	0.0000	0.3136	2nd	9
Hum 1015	5.1896		4.80648	5.092917	0.0967033	0.1044061	0.926223	0.3605	0.3013	0.5333	0.0000	0.3233	0.3048	0.5903	0.5148	0.1574	0.3605	0.1150	1st	2
Hum 1220	5.0454		4.80648	5.092917	0.0475567	0.1044061	0.455497	0.6515	0.0200	0.4560	0.0000	0.0224	0.7356	0.4067	0.0484	0.0076	0.6515	0.0731	1st	6
Hum 1461	5.0370		4.80648	5.092917	0.0559667	0.1044061	0.536048	0.5952	0.0165	0.4096	0.0000	0.0185	0.6763	0.3636	0.0406	0.0062	0.5952	0.0603	1st	6
Hum 1478	5.2439		4.80648	5.092917	0.1509433	0.1044061	1.445733	0.1569	0.7009	0.2582	0.0000	0.6338	0.1274	0.2947	0.8917	0.3621	0.1569	0.0676	1st	2
Hum 1685	5.2852		4.80648	5.092917	0.1923133	0.1044061	1.841974	0.0737	0.8969	0.1310	0.0000	0.9341	0.0582	0.1530	0.7963	0.6023	0.0737	0.0891	1st	5
Hum 1806	5.0239		4.80648	5.092917	0.0690367	0.1044061	0.661233	0.5127	0.0122	0.3437	0.0000	0.0137	0.5884	0.3027	0.0307	0.0044	0.5127	0.0581	1st	7

Table 4.2: Overall Results

Reassociations			
Articulated elements	Number of queries	Correct	Incorrect
Humerus/Radius	18	16	2
Humerus/Ulna	19	15	4
Scapula/Humerus	20	18	2
Femur/Tibia	19	18	1
Tibia/Fibula	19	18	1
Talus/Calcaneus	16	16	0
Tibia/Talus	19	19	0
Femur/Ilium	18	16	2
Total	148	136	12
Percentage	100%	91.89%	8.11%

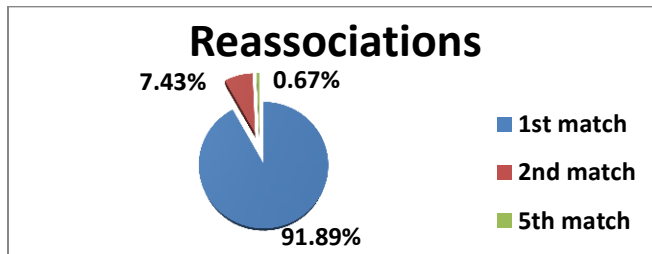


Figure 4.3: Rank of Correct Matches

Hot Spot Analysis

The Hot Spot Analysis of phalanges identified 10 clusters composed of 277 significant cells. Fifteen carpal clusters composed of 216 significant cells were identified. Seven vertebrae clusters composed of 452 significant cells were identified. Eight rib clusters composed of 199 significant cells were identified. Nineteen metapodial clusters composed of 246 significant cells were identified. Figure 4.4 shows the legend used to interpret the Hot Spot Analysis results. Figures 4.5- 4.9 show the results for phalanges, carpals, vertebrae, ribs and metapodials. Accuracy of Hot Spot Analysis for identifying individuals was calculated by quantifying the number of vertebrae or ribs captured in significant cells of clusters. Results show that 73.75% of vertebrae and 76.69% of ribs were spatially clustered (Tables 4.2 and 4.3).

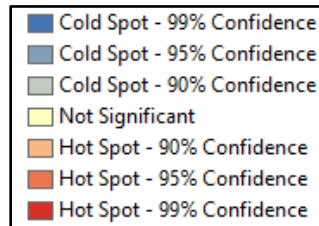


Figure 4.4: Colors that Represent Hot and Cold Cells

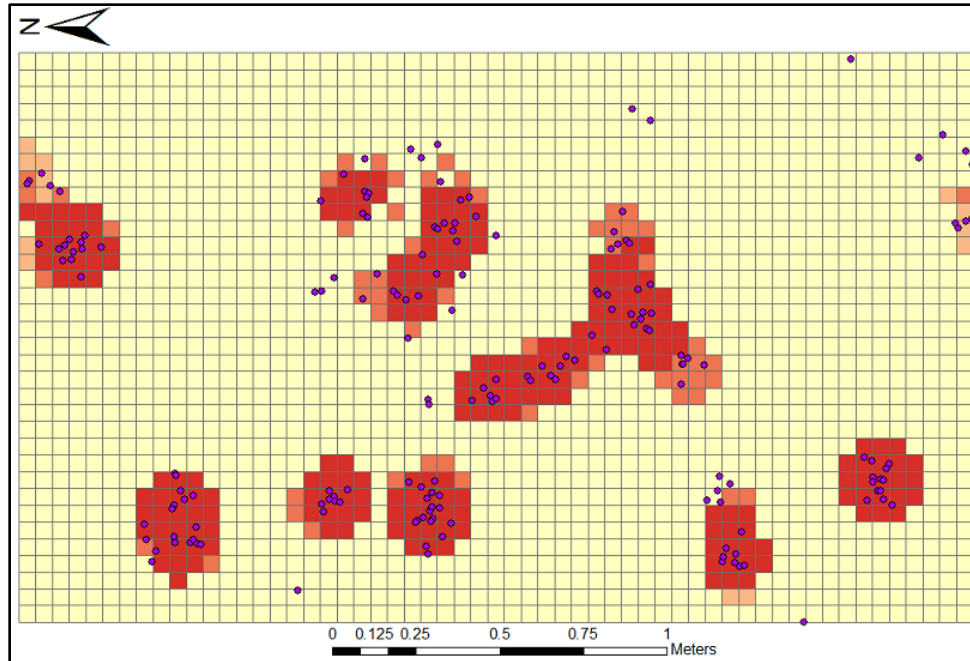


Figure 4.5: Hot Spot Analysis of Phalanges

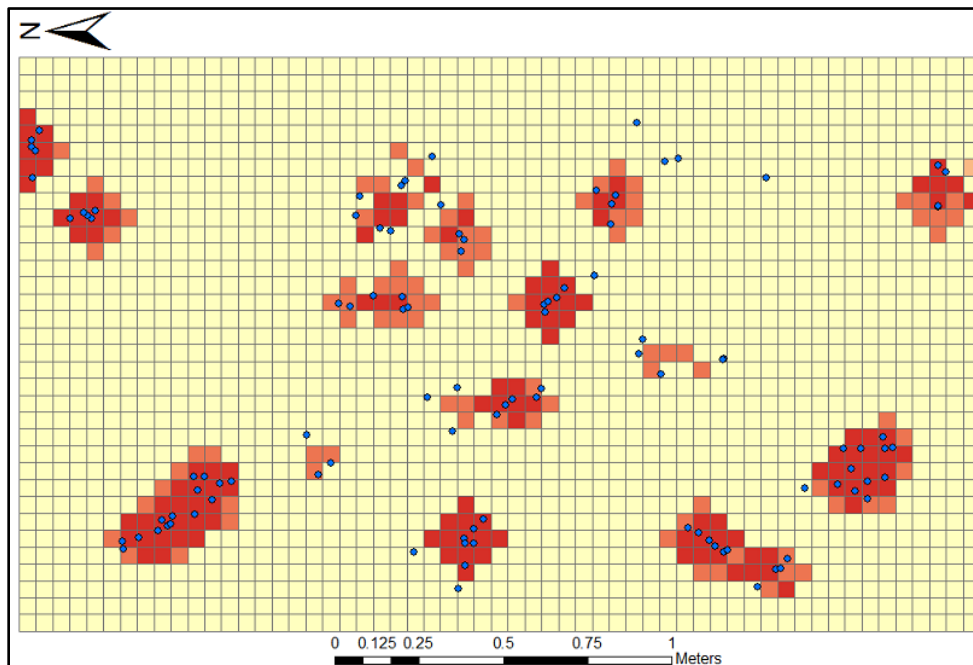


Figure 4.6: Hot Spot Analysis of Carpals

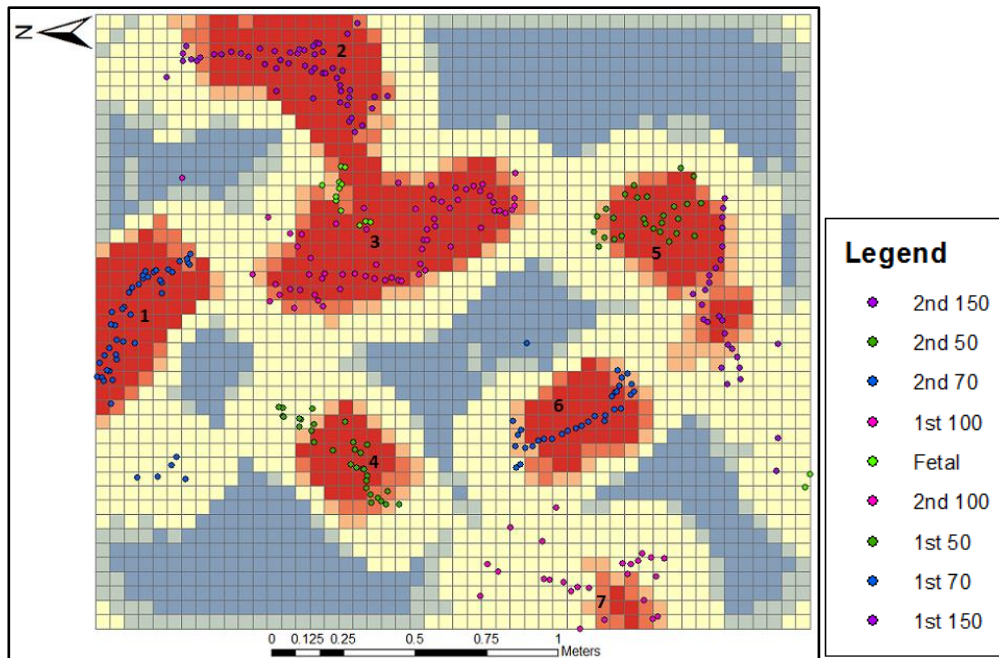


Figure 4.7: Hot Spot Analysis of Vertebrae

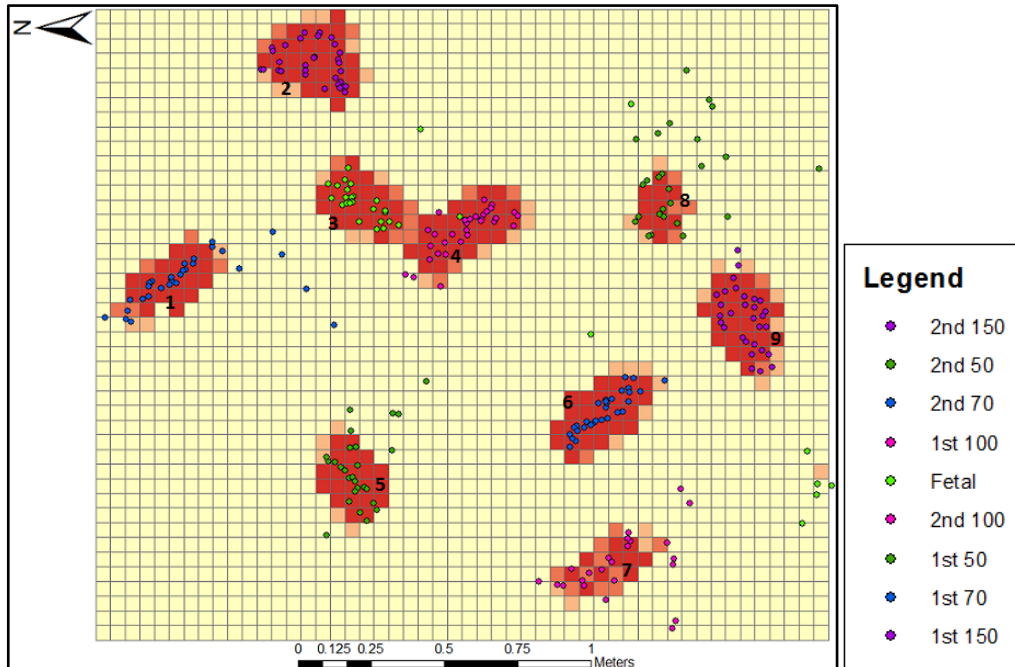


Figure 4.8: Hot Spot Analysis of Ribs

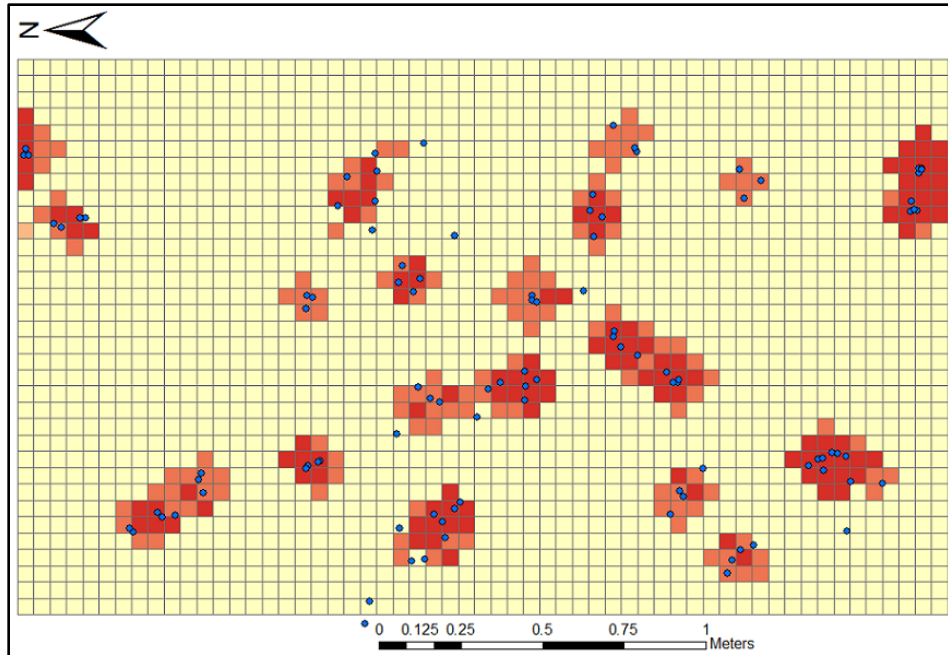


Figure 4.9: Hot Spot Analysis of Metapodials

Table 4.3: Results for Hot Spot Analysis of Vertebrae

Hotspot Analysis of vertebrae				
Pig	Cluster	vertebrae	# in cluster	% correct
1st 70	1	45	40	88.89%
2nd 150	2	52	47	90.38%
1st 100	3	64	59	92.19%
1st Fetal	3	12	10	83.33%
1st 50	4	31	20	64.52%
2nd 50	5	27	22	81.48%
1st 150	5	27	14	51.85%
2nd 70	6	32	20	62.50%
2nd 100	7	28	4	14.29%
2nd Fetal	No cluster	2	0	0.00%
Overall		320	236	73.75%

Table 4.4: Results for Hot Spot Analysis of Ribs

Hotspot Analysis of ribs				
Pig	Cluster	Ribs	# in cluster	% correct
1st 70	1	30	20	66.67%
2nd 150	2	30	28	93.33%
1st Fetal	3	29	26	89.66%
1s 100	4	32	29	90.63%
1st 50	5	27	17	62.96%
2nd 70	6	30	29	96.67%
2nd 100	7	24	14	58.33%
2nd 50	8	26	11	42.31%
1st 150	9	33	30	90.91%
2nd Fetal	No cluster	5	0	0.00%
Overall		266	204	76.69%

II. Results for Osteometric Sorting

While osteometric sorting is used as one of the controls for this project, it can also be compared to spatial analysis as a method for sorting commingled remains. Osteometric sorting was controlled for with visual pair matching and time lapse photography. Results for the accuracy of osteometric sorting were assessed by quantifying the number of bones accurately segregated as well as bones that were not segregated. Overall, bones were segregated or not segregated correctly in 48.17% of comparisons. Results are presented in Table 4.5. Results for each set of comparisons are presented in Appendix I.

Table 4.5: Results for Osteometric Sorting

Osteometric Sorting			
	# of Comparisons	Correct	Percentage
Humerus/Radius	171	93	54.39%
Humerus/Ulna	180	134	74.44%
Scapula/Humerus	190	67	35.26%
Femur/Tibia	171	145	84.80%
Tibia/Fibula	171	125	73.10%
Talus/Calcaneus	153	16	10.46%
Tibia/Talus	152	13	8.55%
Femur/Ilium	180	66	36.67%
Overall	1368	659	48.17%

CHAPTER 5: Discussion

I. Reassociations made with GIS

Near 3D Analysis

Reassociation using spatial analysis should be considered as one of many techniques used to reassociate commingled remains. While the Near 3D analysis resulted in a 91.89% success rate, it cannot confirm, with statistical confidence, each match made based on proximity. Osteometric sorting produces results with statistical confidence levels and visual pair matching permits visual inspection of overall morphology and taphonomic changes. While these methods are useful in situations of small scale commingling they become less useful when the number of individuals increases (Byrd, 2008). The more individuals present the more likely it is that there will be persons with bones of similar size and morphology. For best results in both small and large scale commingling, a method such as Near 3D should be employed in combination with these methods. Used as a first approach, spatial analysis matches skeletal elements based on proximity, which will decrease the number of comparisons that need to be made using osteometric sorting and/or visual pair matching. Each match can be confirmed or repudiated with the other methods. If a match is rejected, the second closest element will be compared and so on. Once a match is accepted one can move on to the next reassociation.

Hot Spot Analysis

Carpals, phalanges and metapodials were not controlled for in the present study. Therefore, accuracy of the results can only be speculated. Ten clusters of phalanges were identified. While there were 10 pigs in the grave, the results were difficult to interpret in this context. Fore and hind limb phalanges look very similar due to the quadrupedal nature of pigs. Limbs overlapped significantly during the initial positioning of pigs in the grave; however, when comparing the cluster analysis to the original position of the pigs it appears that some clusters do belong to specific pigs.

Fifteen carpal and nineteen metapodial clusters were identified. These were also difficult to interpret in this context for the same reason stated above. However, when compared to the original position of the pigs it appears that some clusters belong to certain pigs and even align with specific limbs.

Vertebrae and ribs were controlled for using time lapse photography. Seven vertebrae clusters were identified. Because every unfused element was mapped in the north portion of the grave, the map indicates that clusters in the north portion of the grave have more than 27 (average number of vertebrae in a pig) vertebrae per cluster. Vertebral bodies and arches were mostly unfused and were mapped separately. Therefore the clusters in the north are more numerous but still compose one pig. In the south portion of the grave, only representative portions (the vertebral arcs) of the vertebrae were mapped, so there are an anatomically correct number of vertebrae representing a pig. After segregating vertebrae it was discovered that some vertebrae in cluster 3 were from the 1st fetal pig; therefore, this cluster represents two pigs. Cluster 5 contains the vertebrae of two pigs; the second 50 lb pig

and the second 150 lb pig. From the map in Figure 4.7 and Table 4.2, it is clear that not all of the vertebrae from the second fetal were found to create a cluster. A total of 73.75% of vertebrae were included in the clusters. The remaining vertebrae are in close proximity, but are not included in cells with significant p -values.

Nine rib clusters were identified. These clusters leave out more elements than the vertebral clusters, but are more accurate in identifying individual pigs. Depending on the interpretation of the analyst, clusters 3 and 4 may be combined. However, accounting for the correct number of ribs in the body can assist in determining if the clusters should be separated. In this case it is known that the clusters should be separated as the grouping contains two pigs. Again, not enough ribs from the second fetal pig were found to create a cluster of significant cells; however, an association was identified by one cell indicating moderate clustering. A total of 76.69% of ribs were included in clusters. Ribs not included in clusters were more dispersed compared to the vertebrae.

While some interpretation is necessary, clusters represented individual pigs well. Of most importance, the Hot Spot Analysis produces results based on statistical computations that can be considered quantitative and objective. It addresses the smaller bones that are largely ignored by other reassociation methods. Lastly, because clusters tended to represent individual pigs, Hot Spot Analysis can aid in estimating the MNI.

Quantified Results

A more definite statement about the success of this analysis can be made by examining how much of each subject was reassociated. There are a total of 235 bones in pig

skeleton. This includes 44 teeth and the 26 bones that make up the cranium. In this analysis teeth were not mapped as they were still embedded in bone. Individual bones of the cranium were also not mapped as a cranium was collected as one element. For the purposes of this research 166 bones make up a complete skeleton. Accurate reassociations could only be made with the Near 3D and Hotspot Analyses of ribs and vertebrae. Hotspot Analysis clusters of carpals, metapodials and phalanges were associated with individual pigs based on location in the grave. The most complete subject was the first 150 lb pig with 46.99% of elements reassociated with controlled analyses and 92.77% of elements reassociated with all analyses. Results for the remaining subjects can be found in Table 5.1.

Table 5.1: Quantified Results

Subject	# of elements (controlled)	% found	# of elements (total)	% found
1st Fetal	58	34.94%	74	44.58%
2nd Fetal	14	8.43%	15	9.04%
1st 50 lb	75	45.18%	124	74.69%
2nd 50 lb	74	44.58%	100	60.24%
1st 70 lb	79	47.59%	117	70.48%
2nd 70 lb	78	46.99%	135	81.33%
1st 100 lb	79	47.59%	152	91.57%
2nd 100 lb	73	45.78%	143	86.14%
1st 150 lb	78	46.99%	154	92.77%
2nd 150 lb	79	47.59%	139	83.73%

II. Comparison of Methods: Osteometric Sorting

Osteometric sorting was successful in 48.17% of comparisons. While there is a large amount of size variation in the study sample, it should be recognized that there are only five different weights. Two pigs of each size were used and placed on opposite sides of the grave; therefore, at least two bones from each group analyzed may be too similar to sort. Isometric relationships exist between all bones in the skeleton; however, some are much stronger than others (Byrd, 2008). Femora with tibiae were sorted with the highest success at 84.80%. There are also high accuracy rates among other long bones such as the humerus and ulna (74.44%) and the tibia and fibula (73.10%). This is expected as it is known that strong correlations exist between long bone lengths (Trotter & Gleser, 1952; Byrd & Adams, 2003). For scapulae, tali, calcanei and ilia, size relationships appear to be weaker. The R^2 value or coefficient of determination, for each regression reflects how well one variable explains the other. The R^2 values for the regression models used in this study are presented in Table 5.2. As expected, R^2 for humerus on ulna, tibia on femur and fibula on tibia are the highest. While the R^2 for radius on humerus is only .0042 lower than tibia on femur, the model performs poorly. This shows how strong the isometric relationship between two bones must be for osteometric sorting to be successful. Also, such relationships may only exist between certain bones such as the humerus, ulna, tibia, femur and fibula.

Table 5.2: R² Values for Each Regression Model

Regression Model	R ²
Radius on Humerus	0.9894
Humerus on Scapula	0.9689
Humerus on Ulna	0.9944
Tibia on Femur	0.9977
Fibula on Tibia	0.9936
Calcaneous on Talus	0.5115
Talus on Tibia	0.8231
Ilium on Femur	0.9576

The effectiveness of osteometric sorting depends on a number of criteria. Much size variation must exist in the population in question, there must be a large and diverse sample size and the reference population should be similar to the population in question (Byrd, 2008, Chew, 2014). While, the first criterion is covered here because the study sample was chosen for its large size variation, the reference sample used was composed of only 48 incomplete observations; some pig skeletons were missing bones. Reference sample size varied between 28 and 41 observations for different sets of comparisons. This is rather small compared to the reference sample of 316 observations used by Byrd & Adams (2003). The reference sample for this study (collected from various sources) was composed of pigs from different countries and time periods. Studies have identified significant size variation between pigs from different geographic regions and time periods (Albarella, 2009). This was revealed to be a problem when using the Forensic Databank (a modern American sample) as a reference sample for a Native American archaeological sample (Chew, 2014). These issues likely affected the osteometric sorting. When compared, the success rate for spatial analysis in the

reassociation of commingled remains in this study was 43.72% higher than the success rate of osteometric sorting.

III. The Mapping Process

The overall amount of time taken to map the grave was 14 days. The grave measured approximately 10 x 8 ½ ft and contained 10 individuals. This is a rather small endeavor in comparison to a mass grave measuring 82 x 8 ft containing 289 individuals (Tuller et al., 2008). Translating this method to a mass grave of this size and capacity may not seem practical. However, for this project the number of people helping ranged from two-six. More than half of the time only two people were available to map. If four people (the ideal number to employ the mapping process) were available every day, the process may have been much quicker. Two different mapping strategies were employed. In the north portion of the grave, every element was mapped. This included epiphysis, fragments and sesamoid bones as well as un-fused portions. This lengthened the process substantially. In the south portion of the grave these elements were omitted, which would be more comparable to a mass grave containing fewer juveniles with little fragmentation. In this study every coordinate taken was read aloud and manually recorded. This was done to account for potential user error. The total station records every point, but the user must press 'Record'. In the present study, this was important because most users were inexperienced. A number of points had to be corrected using the manual bone log due to user errors with the machine. While mapping a site with a total station is much quicker than using traditional hand measurements, the strategy can be improved further. For the most efficient process, it is

suggested that four to five people be employed to map the grave in its entirety, extraneous elements are not mapped and coordinates are recorded only with the total station. Another way to speed up the process would be using an external keyboard with the total station so codes can be quickly typed in and recorded. Typically the user must scroll through a list of codes saved in the total station every time a different point is recorded.

Not all the codes used in this analysis were found to be of use for reassociation. It is suggested that these codes be excluded when implementing this method in a real scenario. Only one measurement should be taken on the cranium, mandible and portions of the os coxa. Codes EPIP, OCX4, OCCR, OCCL, EPIP, and MANL or MANR were extraneous and should be removed. If types of vertebrae can be identified in the field quickly it would be helpful to record them with a separate code, for example CERV for cervical vertebrae. This would help to confirm the associations for clusters of vertebrae found in the Hotspot Analysis. If metacarpals and metatarsals can be differentiated they should also receive their own code. If bones can be sided quickly in the field, this should also be included in the code or recorded separately as it saves time during post processing. Table 5.3 contains the codes that should be used for an efficient analysis.

Table 5.3: Suggested Codes

CRAN - cranium, taken on the middle of the basilar area	PFEM - proximal femur, taken at proximal articular surface
VERT - vertebrae, taken at middle of exposed bone	DFEM - distal femur, taken at distal articular surface
CERV - cervical vertebra, taken at middle of exposed bone	PATL - patella, taken at middle of exposed bone
THVT - Thoracic vertebra, taken at middle of exposed bone	PTIB - proximal tibia, taken at proximal articular surface
LUMB - lumbar vertebra, taken at middle of exposed bone	DTIB - distal tibia, taken at distal articular surface
SCAP - scapula, taken at middle of glenoid fossa	PFIB - proximal fibula, taken at proximal articular surface
RIBH - rib, point taken at costal facet, or head	DFIB - distal fibula, taken at distal articular surface
RIBS - rib, point taken and sternal end	TALU - talus, taken at middle of exposed bone
PHUM - proximal humerus, taken at middle of proximal articular surface	CALC - calcaneus, taken as close to articular surface as possible
DHUM - distal humerus, taken at middle of distal articular humerus	OCX1 - os coxa, taken at middle of sacro-iliac joint
PRAD - proximal radius, taken at middle of proximal articular surface	OCX2 - os coxa, taken at mid acetabulum
DRAD - distal radius, taken at middle of distal articular surface	OCX3 - os coxa, taken at middle of pubic symphysis
PULN - proximal ulna, taken at proximal articular surface	STER - Sternum, taken from middle of exposed bone
DULN - distal ulna, taken at distal articular surface	MAND - mandible, taken at the central incisors
METT - Metatarsal, taken at middle of bone	CARP - for both carpals and tarsals, taken and middle of exposed bone
METC - Metacarpal, taken at middle of bone	PHAL - Phalanx, taken from center of exposed bone

IV. Limitations

This method associates left and right sides separately; therefore, other measures must be taken to reassociate left and right sides. A separate model of osteometric sorting which compares paired elements can be used to reassociate left and right sides (Byrd, 2008):

$$\mathbf{D} = \Sigma (\mathbf{a}_i - \mathbf{b}_i).$$

In this model, \mathbf{a} is the right side bone measurement \mathbf{i} , and \mathbf{b} is the left side bone measurement \mathbf{i} for each of the measurements included in the comparison. The null hypothesis states that there is no significant difference between the two elements. It is tested by comparing the value of \mathbf{D} against “0”, which indicates no difference. This model of osteometric sorting can be used in tandem with visual pair matching.

The method tested in this study focused on reassociating previously articulated elements. Due to the maturity of the pigs, many bones were unfused. This was not a problem for easily identifiable elements such as long bones or portions of the os coxae. However, specific vertebrae, especially when fragmentary, could not be identified. This prevented certain skeletal elements from being reassociated. For example, the first cervical vertebra articulates with the cranium. Because first cervical vertebrae were not identified they could not be reassociated with crania. Bones must be accurately identified in order to reassociate them with the correct element. It is because of this that Hot Spot Analysis, instead of Near 3D was used to identify spatially associated clusters of vertebrae, ribs, phalanges, carpals and metapodials. In a previous study, crania were reassociated with the

superior points of full vertebral columns (Tuller et al., 2008). This is recommended when articulated vertebral columns are present and 1st cervical vertebrae can be identified.

The skeletal commingling created for this study represented surface scatter. Buried remains take months or even years to decompose depending on the environment (Ubelaker, 1997). The time frame for this thesis did not allow the time needed for buried remains to decompose and commingle. Placing the pigs on the ground surface permitted time for decomposition as well as natural processes to take place which moved the bones. While perpetrators frequently bury victims in order to hide their crimes, surface scatter of remains occurs as well. For example, PHR conducted an investigation of surface scatter and buried remains at Kibuye Catholic Church after the Rwandan Genocide (Haglund et al., 2001). The present study serves to demonstrate the protocol for applying spatial analysis to a commingled assemblage of remains that have been found in situ. In order to employ the method, remains must be mapped in their original context, be it surface scatter or excavated burial.

Another limitation to consider is the use of proprietary software. ArcGIS has a licensing cost that may be prohibitive. However, spatial analysis can be conducted in a number of GIS programs. It is appropriate to highlight an open source program that is capable of conducting the analysis and presenting the data. GRASS is an open source GIS program that can even be used without an internet connection. In order to conduct the analysis in GRASS the total station points must be saved as a CSV file. The CSV file can be uploaded into GRASS using the `v.in.ascii` command. Coordinate types (e.g. left distal humerus) must be separated in different vector files, or groups. The command `v.distance`

locates the nearest elements in a 'to' vector map for elements in a 'from' vector map. For example the 'to' vector map would be left distal humerus and the 'from' vector map would be left proximal radius. This is essentially, the identical to the Near 3D feature in ArcGIS. A map of the mass grave created in GRASS is shown in Figure 5.1.

While ArcMap is limited, both GRASS and ArcScene, another program in the ArcGIS suite, are useful for working with and displaying 3d vector data. The data can be rotated around and viewed from any angle. Animations can be made to illustrate relationships among certain points in 3D.

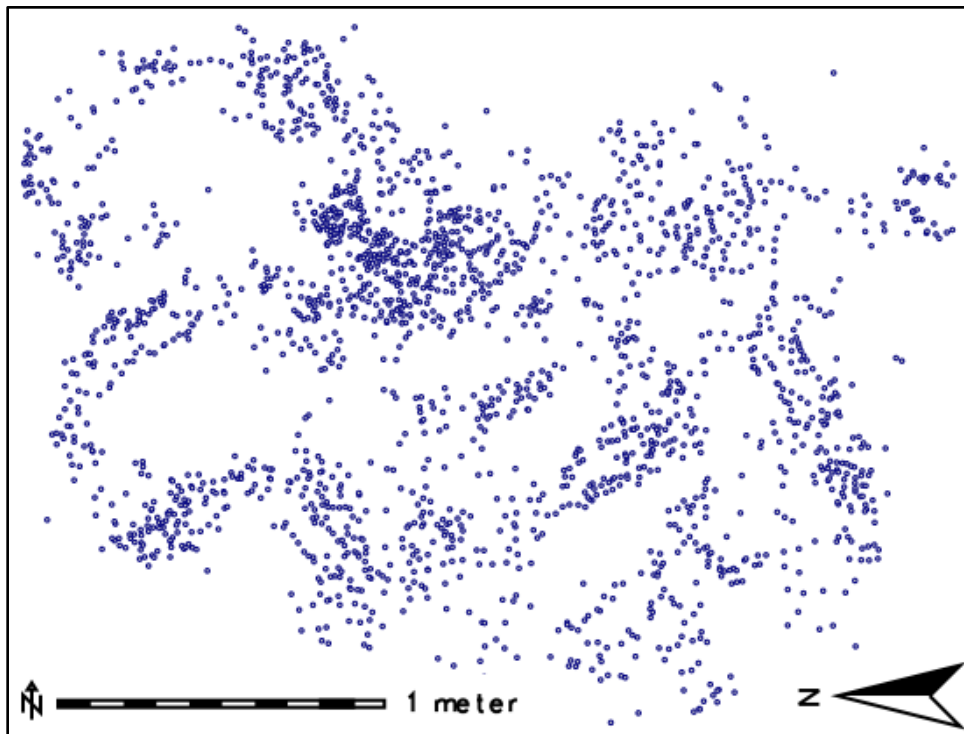


Figure 5.1: A Map of the Mass Grave Created in GRASS

CHAPTER 6: Conclusion

The findings of this research show that spatial analysis should be one of the techniques used to reassociate commingled remains. It is most useful when employed first and then followed by other methods. Using spatial analysis first will reduce the number of comparisons that need to be made with osteometric sorting or visual pair matching, which will hasten the reassociation process. It has the potential to be particularly useful in a large scale commingling when metric and visual methods are more difficult to employ and in commingling situations where DNA comparisons are not an option. A method such as Hot Spot Analysis should be employed for the commingling of highly fragmented assemblages or small skeletal elements that are not addressed by other methods.

Reassociations made with the Near 3D analysis were correct in 91.89% of cases. It performed 43.72% better than osteometric sorting, which is one of the only statistical and thus objective reassociation methods. Hot Spot Analysis succeeded in identifying clusters of vertebrae and ribs that contained individual pigs. While interpretation of the clusters requires a human element such as knowledge of human osteology, on average 75.22% of vertebrae and ribs were spatially clustered. Both spatial analysis methods used in this study are quantitative, objective and display high accuracy rates. This is useful for court room purposes as the methods used by scientists must be tested to show known error rates.

A practical implementation of this method should involve mapping the remains in situ using a device such as a total station. To map with minimal error, the operator of the total station should be experienced especially if the project requires numerous machine set ups.

Articular areas of bones should be recorded, using either the codes in this study or codes developed with another specific purpose. The use of an external keyboard is encouraged if using a total station. Points should be downloaded from the total station to an excel file on the computer and then uploaded to ArcGIS, GRASS or another available GIS program. Articular categories such as left proximal humerus should be separated. A function such as Near 3D or v.distance should be used to query the distance of one set of elements to its set of counterpart elements. The output from this function will indicate the closest missing elements for each set.

Future Considerations

Future research should focus on decreasing the time it takes to map elements accurately and in situ. As technology develops this could include using devices other than the total station. Another factor to consider would be developing standard locations on the bone for mapping so the size of the element can be recreated. This would entail identifying measurements that can be taken on a bone when it is lying in any given position as commingling is often in the form of unpredictable and complex assemblages. New technology should be continuously applied to improve methods of mapping and reassociating commingled remains.

Beyond the reassociation of commingled remains, spatial data can be used to recreate any aspect of the crime scene. If buildings, trees, and artifacts etc. are also mapped, spatial relationships between the surrounding areas, pieces of evidence and remains can be assessed. Maps that are precisely to scale can be created representing the crime scene. This is useful to

investigators if they need to recreate a crime scene in court months or even years in the future. The method can also be employed in a bioarchaeological setting. Mapping remains and artifacts in context is not only useful for reassociating commingled skeletal elements but for site interpretation as well as preservation once the site has been destroyed.

LITERATURE CITED

- About the ICTY, <http://www.icty.org/sections/AbouttheICTY>
- Adams, B. J., & Byrd, J. E. (2006). Resolution of small-scale commingling: A case report from the Vietnam War. *Forensic Science International*, 156(1), 63-69.
- Adams, B. J., & Konigsberg, L. W. (2004). Estimation of the most likely number of individuals from commingled human skeletal remains. *American Journal of Physical Anthropology*, 125(2), 138-151.
- Aerssens, J., Boonen, S., Lowet, G., & Dequeker, J. (1998). Interspecies differences in bone composition, density, and quality: Potential implications for in vivo bone research 1. *Endocrinology*, 139(2), 663-670.
- Agosto, E., Ajmar, A., Boccardo, P., Giulio Tonolo, F., & Lingua, A. (2008). Crime scene reconstruction using a fully geomatic approach. *Sensors*, 8(10), 6280-6302.
- Albarella, U., Dobney, K., & Rowley-Conwy, P. (2009). Size and shape of the eurasian wild boar (*sus scrofa*), with a view to the reconstruction of its holocene history. *Environmental Archaeology*, 14(2), 103-136.
- Aumaitre, A., Sybesma, W., Vanderhaegen, J., Whittemore, C., & Zivkovic, S. (1982). IV. Pigs. *Livestock Production Science*, 9(1-2), 127-161.
- Baker, P. T., & Newman, R. W. (1957). The use of bone weight for human identification. *American Journal of Physical Anthropology*, 15(4), 601-618.
doi:10.1002/ajpa.1330150410
- Behrensmeyer, A. K. (1978). Taphonomic and ecologic information from bone weathering. *Paleobiology*, 150-162.
- Bernatchez, J., & Marean, C. W. (2011). Total station archaeology and the use of digital photography. *SAA Archaeol. Rec*, 11, 16-21.
- Binford, L. R. (1977). *For theory building in archaeology: Essays on faunal remains, aquatic resources, spatial analysis, and systemic modeling* Academic Pr.
- Blum, R., Stanton, G. H., Sagi, S., & Richter, E. D. (2008). 'Ethnic cleansing' bleaches the atrocities of genocide. *European Journal of Public Health*, 18(2), 204-209.
- Buchli, V., Lucas, G., & Cox, M. (2001). *Archaeologies of the contemporary past*. London: Routledge. Chapter 12: Science and Human Rights. 138-144 p.

- Buergenthal, T. (1994). United nations truth commission for el salvador, the. *Vand.J.Transnat'l L.*, 27, 497.
- Buikstra, J. E., & Gordon, C. C. (1980). Individuation in forensic science study: Decapitation. *Journal of Forensic Sciences*, 25(1), 246-259.
- Burns, K. R. (1999). *Forensic anthropology training manual*. Upper Saddle River, N.J: Prentice Hall. Chapter 3: Forensic Anthropology and Human Rights Issues. 63-85 p.
- Byrd, J. E. (2008). Models and methods for osteometric sorting. Recovery, analysis, and identification of commingled human remains (pp. 199-220) Springer.
- Byrd, John E. & Adams, Bradley J. (2003). "Osteometric sorting of commingled human remains". *Journal of forensic sciences* (0022-1198), 48 (4), 717 p.
- Adams, B. J., & Byrd, J. E. (2006). Resolution of small-scale commingling: A case report from the Vietnam war. *Forensic Science International*, 156(1), 63-69.
- Byrd, J. H., & Castner, J. L. (2012). *Forensic entomology: The utility of arthropods in legal investigations* CRC press.
- Cabo, L. L., Dirkmaat, D. C., Adovasio, J. M., & Rozas, V. C. (2012). Archaeology, mass graves, and resolving commingling issues through spatial analysis. A companion to forensic anthropology (pp. 175-196) John Wiley & Sons, Ltd. doi:10.1002/9781118255377.ch9
- Cabo, L. L. (2012). DNA analysis and the classic goal of forensic anthropology. A Companion to Forensic Anthropology, 447-461.
- Caplan, P. (2007). Never again? : Genocide memorials in Rwanda. *Anthropology Today*, 23(1), 20-22. doi:10.1111/j.1467-8322.2007.00486.x
- Catts, E. (1992). Problems in estimating the postmortem interval in death investigations. *Journal of Agricultural Entomology*, 9(4), 245-255.
- Chainey, S., & Ratcliffe, J. (2005). *GIS and crime mapping*. John Wiley & Sons.
- Chan, Y. (2011). A software survey of analytics and spatial information technology. Location theory and decision analysis (pp. 411-440) Springer.
- Chew, K. R. (2014). The use of osteometric sorting techniques to aid in the resolution of a large scale commingling: The piggot ossuary site (31CR14).

- Cordner, S., & Coupland, R. (2003). Missing people and mass graves in Iraq. *The Lancet*, 362(9392), 1325-1326.
- Crossland, Z. (2013). Evidential regimes of forensic archaeology*. *Annual Review of Anthropology*, 42, 121-137.
- Cunningham, S. L., Kirkland, S. A., & Ross, A. H. (2011). Bone weathering of juvenile-sized remains in the north carolina piedmont. *The juvenile skeleton in forensic abuse investigations* (pp. 179-196) Springer.
- Dirkmaat, D. C., Cabo, L. L., Adovasio, J. M., & Rozas, V. (2007). Commingled remains and the mass grave.
- EAAF (2007) "Argentina" EAAF Annual Report.
http://eaaf.typepad.com/annual_report_2007/An07_Argentina-8.pdf
- Eyman, C. E. (1965). Ultraviolet fluorescence as a means of skeletal identification. *American Antiquity*, 31(1), 109-112. Retrieved from
<http://www.jstor.org.prox.lib.ncsu.edu/stable/2694031>
- Finnegan, M., & Chaudhuri, S. (1990). Identification of commingled skeletal remains using isotopic strontium. Paper presented at the 42nd Annual Meeting of the American Academy of Forensic Science, Cincinnati, OH
- Freud, R. J., & Littell, R. C. (2000). SAS system for regression Sas Institute.
- Fulton, B. A., Meloen, C. E., & Finnegan, M. (1986). Reassembling scattered and mixed human bones by trace element ratios. *Journal of forensic sciences*, 31(4), 1455-1462.
- Gardner, R., & Bevel, T. (2009). CH. 11 Developing and Using Demonstrative Exhibits in Support of the Crime Scene Analysis. In *Practical crime scene analysis and reconstruction*. CRC Press.
- General Assembly (1996), REPORT OF THE INTERNATIONAL TRIBUNAL FOR THE PROSECUTION OF PERSONS RESPONSIBLE FOR SERIOUS VIOLATIONS OF INTERNATIONAL HUMANITARIAN LAW COMMITTED IN THE TERRITORY OF THE FORMER YUGOSLAVIA SINCE 1991. Retrieved December 12, 2014, from [http://www.icty.org/x/file/About/Reports and Publications/AnnualReports/annual_report_1996_en.pdf](http://www.icty.org/x/file/About/Reports%20and%20Publications/AnnualReports/annual_report_1996_en.pdf)
- GIS Dictionary. Retrieved December 8, 2014, from
<http://support.esri.com/en/knowledgebase/Gisdictionary/browse>

- Haglund, W. D., & Sorg, M. H. (Eds.). (1997). *Forensic taphonomy: the postmortem fate of human remains*. CRC Press.
- Haglund, W.D., Connor, M. & Scott, D.D., (2001). The Archaeology of Contemporary Mass Graves. *Historical Archaeology*, Vol. 35, No. 1, Archaeologists as Forensic Investigators: Defining the Role, pp. 57-69
- Hale, A.R. & Ross, A. H., (2015, February) An Innovative Analysis of the Postmortem Interval and Its Role in Juvenile Decomposition. Poster presented at the American Academy of Forensic Science, Orlando, FL.
- Hall, G. B., & Leahy, M. G. (2008). Chapter 9 Grass GIS. *Open source approaches in spatial data handling* Springer.
- Hillson, S. (1999). *Mammal bones and teeth: An introductory guide to methods of identification* Institute of Archaeology. p 46.
- History of the EAAF, http://eaaf.typepad.com/founding_of_eaaf/
- Holland, M. M., Fisher, D. L., Mitchell, L. G., Rodriquez, W. C., Canik, J. J., Merrill, C. R., & Weedn, V. W. (1993). Mitochondrial DNA sequence analysis of human skeletal remains: identification of remains from the Vietnam War. *Journal of forensic sciences*, 38(3), 542-553.
- Honeycutt, Kenda K. (2012) "Fracture Patterns and Taphonomic Processes in a Mass Grave Environment: A Quantitative Analysis."
- Human Rights Watch (2013) "Mexico: Build Accurate Database of Disappeared." Web. 8 Dec. 2013. <<http://www.hrw.org/news/2013/11/12/mexico-build-accurate-database-disappeared>>.
- ICTY, United Nations International Criminal Tribunal for the Former Yugoslavia. (2000) "SREBRENICA Srebrenica Investigation: Summary of Forensic Evidence-Execution Points and Mass Graves"
http://www.domovina.net/archive/2000/20000516_manning.pdf
- Iqbal, K. (2012). THE DIS-UNITED NATIONS. *Defence Journal*, 16(3), 3-1J,2J,3J.
Retrieved from
<http://proxying.lib.ncsu.edu/index.php?url=/docview/1189877063?accountid=12725>
- International Criminal Tribunal for the Former Yugoslavia (ICTY), 1996.
- Jessee, E., & Skinner, M. (2005). A typology of mass grave and mass grave-related sites. *Forensic science international*, 152(1), 55-59.

- Kerley, E. R. 1972 Special observations in skeletal identification. *J. Forensic Sci.* 17(3):349–357.
- Kohut, D. R., & Vilella, O. (2010). *Historical dictionary of the "dirty wars"*. Lanham: Scarecrow Press. pg 150-152
- Komar, D. A., & Buikstra, J. E. (2008). *Forensic anthropology: contemporary theory and practice*. Oxford University Press.
- L'Abbe, E. N. 2005 A case of commingled remains from rural South Africa. *Forensic Sci. Int.* 151(2–3):201–206.
- Listi, G. A., Manhein, M. H., & Leitner, M. (2007). Use of the global positioning system in the field recovery of scattered human remains*. *Journal of Forensic Sciences*, 52(1), 11-15.
- Little, C. Q., Small, D. E., Peters, R. R., & Rigdon, J. B. (2000). Forensic 3D scene reconstruction. Paper presented at the 28th AIPR Workshop: 3D Visualization for Data Exploration and Decision Making, 67-73.
- London, M. R. and B. K. Curran (1986). The use of the hip joint in the separation of commingled remains (abstract). *Am. J. Phys. Anthropol.* 69:231
- London, M. R. and D. R. Hunt (1998). Morphometric segregation of commingled remains using the femoral head and acetabulum (abstract). *Am. J. Phys. Anthropol.* 26(Suppl):152
- Marean, C. W., Abe, Y., Nilssen, P. J., & Stone, E. C. (2001). Estimating the minimum number of skeletal elements (MNE) in zooarchaeology: a review and a new image-analysis GIS approach. *American Antiquity*, 333-348.
- Maxwell, A., & Ross, A. H. (2011). Epidemiology of Genocide: An Example from the Former Yugoslavia. *Forensic Science Policy & Management: An International Journal*, 2(2), 94-102.
- McPherron, S. J. (2005). Artifact orientations and site formation processes from total station proveniences. *Journal of Archaeological Science*, 32(7), 1003-1014.
- McPherron, S. P., & Dibble, H. L. (2002). *Using computers in archaeology: A practical guide* McGraw-Hill Humanities/Social Sciences/Languages.
- McKern, T. W. (1958). The use of Short Wave Ultra-Violet Rays for the Segregation of Commingled Skeletal Remains

- Manhein, M. H., Listi, G. A., & Leitner, M. (2006). The application of geographic information systems and spatial analysis to assess dumped and subsequently scattered human remains. *Journal of Forensic Sciences*, 51(3), 469-474.
- Mettraux, G. (2005). *International crimes and the ad hoc tribunals* Oxford University Press.
- Mundorff, A. Z., Shaler, R., Bieschke, E., & Mar-Cash, E. (2008). Marrying anthropology and DNA: Essential for solving complex commingling problems in cases of extreme fragmentation. *Recovery, analysis, and identification of commingled human remains* (pp. 285-299) Springer.
- Mundorff, A. (2012). Integrating forensic anthropology into disaster victim identification. *Forensic Science, Medicine and Pathology*, Volume 8, Number 2 (2012), 131-139
- Munsell, A. H., & Color, M. (2000). *Munsell soil color charts* Munsell Color.
- National Institute of Justice. "Using DNA to Solve Cold Cases." July 2002. www.ncjrs.gov/pdffiles1/nij/194197.pdf
- Nee, J., Carson, J. L., & Legg, B. (1997). Technology transfer success story: Total station use for accident investigation. *ITE Journal*, 67(6), 24-26.
- Neubauer, W. (2004). GIS in archaeology—the interface between prospection and excavation. *Archaeological Prospection*, 11(3), 159-166.
- Neuffer, E. (1999). Mass Graves. *Nieman Reports*, 53(2), 9.
- Newbury, C. (1995). Background to genocide: Rwanda. *Issue: A Journal of Opinion*, 12-17.
- Nielsen, K. L., Hartvigsen, M. L., Hedemann, M. S., Laerke, H. N., Hermansen, K., & Bach Knudsen, K. E. (2014). Similar metabolic responses in pigs and humans to breads with different contents and compositions of dietary fibers: A metabolomics study. *The American Journal of Clinical Nutrition*, 99(4), 941-949.
- Nigro, J. D., Ungar, P. S., de Ruiter, D. J., & Berger, L. R. (2003). Developing a geographic information system (GIS) for mapping and analyzing fossil deposits at Swartkrans, Gauteng Province, South Africa. *Journal of Archaeological Science*, 30(3), 317-324.
- North Carolina Department of Transportation (NCDOT) (2012). *Archaeological Predictive Modeling*. Retrieved from http://environment.fhwa.dot.gov/histpres/nc_arch.asp
- Office of the UN Special Advisor on the Prevention of Genocide (OSAPG), (2014) https://www.un.org/en/preventgenocide/adviser/pdf/osapg_analysis_framework.pdf

- Operator's Manual. (2002). Retrieved December 13, 2014, from http://www.glm-laser.com/glm/files/sokkia_setx10_instruction_manual.pdf
- Ord, J. K., & Getis, A. (1995). Local spatial autocorrelation statistics: Distributional issues and an application. *Geographical Analysis*, 27(4), 286-306.
- Owsley, D. W., D. H. Ubelaker, M. M. Houck, K. L. Sandness, W. E. Grant, E. A. Craig, T. J. Woltanski, and N. Peerwani (1995) The role of forensic anthropology in the recovery and analysis of Branch Davidian Compound victims: Techniques of analysis. *J. Forensic Sci.* 40(3):341–348.
- Patterson, J. K., Lei, X. G., & Miller, D. D. (2008). The pig as an experimental model for elucidating the mechanisms governing dietary influence on mineral absorption. *Experimental Biology and Medicine* (Maywood, N.J.),233(6), 651-664.
- Perechocky, A. (2014). Los torturadores medicos: Medical collusion with human rights abuses in Argentina, 1976–1983. *Journal of Bioethical Inquiry*, 11(4), 539-551.
- Robinson, M. (1998). The universal declaration of human rights: Hope and history. *Health and Human Rights*, 27-29.
- Rotberg, R. I., & Thompson, D. (2010). *Truth v. justice: The morality of truth commissions: The morality of truth commissions* Princeton University Press.
- Ross, A. H., & Cunningham, S. L. (2011). Time-since-death and bone weathering in a tropical environment. *Forensic Science International*, 204(1), 126-133.
- Rwanda after the genocide, http://yale.edu/gsp/rwanda/rwanda_after_genocide.html
- Sarkin, J. (1999). The necessity and challenges of establishing a truth and reconciliation commission in Rwanda. *Human Rights Quarterly*, 767-823.
- Schabas, W. (2006). *The UN international criminal tribunals* Cambridge University Press.
- Schoenly, K. G., Haskell, N. H., Mills, D. K., Bieme-Ndi, C., Larsen, K., & Lee, Y. (2006). Recreating death's acre in the school yard: using pig carcasses as model corpses to teach concepts of forensic entomology & ecological succession. *The American Biology Teacher*, 68(7), 402-410.
- Skinner M. (1987), *Planning the Archaeological Recovery of Evidence from Recent Mass Graves*
- Sládek, V., Galeta, P., & Sosna, D. (2012). Measuring human remains in the field: Grid technique, total station, or MicroScribe? *Forensic Science International*, 221(1), 16-22.

- Snow, C. C., Levine, L. J., Lukash, L., Tedeschi, L. G., Orrego, C., & Stover, E. (1984). The investigation of the human remains of the "disappeared" in Argentina. *The American journal of forensic medicine and pathology*, 5(4), 297-299.
- Snow, C. C., & Folk, E. D. (1970). Statistical assessment of commingled skeletal remains. *American journal of physical anthropology*, 32(3), 423-427.
- Snow, C. (1995). Murder most foul. *The Sciences*, 35(3), 16-20.
- Steadman, D. W., & Haglund, W. D. (2005). The scope of anthropological contributions to human rights investigations. *Journal of Forensic Sciences*, 50(1), 23-30.
- Steele C. (2008). Archaeology and the Forensic Investigation of Recent Mass Graves: Ethical Issues for a New Practice of Archaeology. *Archaeologies: Journal of the World Archaeological Congress*, [Volume 4, Number 3](#) (2008), 414-428
- Steiniger, S., & Hunter, A. J. (2013). The 2012 free and open source GIS software map—A guide to facilitate research, development, and adoption. *Computers, Environment and Urban Systems*, 39, 136-150.
- Stover, E., & Peress, G. (1998). *The graves: Srebrenica and vukovar* Scalo Verlag Ac.
- Tersigni-Tarrant, M. A., & Shirley, N. R. (2013). *Forensic anthropology: An introduction* CRC Press.
- Tobler, W. R. (1970). A computer movie simulating urban growth in the Detroit region. *Economic geography*, 234-240.
- Trotter, M., & Gleser, G. C. (1952). Estimation of stature from long bones of american whites and negroes. *American Journal of Physical Anthropology*, 10(4), 463-514.
- Tuller, H., Hofmeister, U., & Daley, S. (2008). Spatial analysis of mass grave mapping data to assist in the re-association of disarticulated and commingled human remains. In *Recovery, analysis, and identification of commingled human remains* (pp. 7-29). Humana Press.
- Turner, S., Doretti, M., & Bernardi, P. (2008). Commingled remains and human rights investigations. *Recovery, analysis, and identification of commingled human remains* (pp. 57-80) Springer.
- Ubelaker, D. H. (1997). Taphonomic applications in forensic anthropology. Hagelund, D./Sorg, M.: *Forensic taphonomy: the postmortem fate of human remains*.

- Ubelaker, D. H. (2008). Methodology in commingling analysis: An historical overview. Recovery, analysis, and identification of commingled human remains (pp. 1-6) Springer.
- UN (1948) The Universal Declaration of Human Rights, <http://www.un.org/en/documents/udhr/index.shtml>
- UN (1948) “Convention on the Prevention and Punishment of the Crime of Genocide”
- UN (1992) “Declaration on the Protection of All Persons from Enforced Disappearance”
- UN (1998) “Diplomatic Conference of Plenipotentiaries on the Establishment of an International Criminal Court” <http://legal.un.org/diplomaticconferences/icc-1998/icc-1998.html>
- Verwimp, P. (2004). Death and survival during the 1994 genocide in Rwanda. Population Studies, 58(2), 233-245.
- Von Den Driesch, A. (1976). A guide to the measurement of animal bones from archaeological sites: As developed by the institut für palaeoanatomie, domestikationsforschung und geschichte der tiermedizin of the university of munich Peabody Museum Press.
- Weaver, M., Sorenson, F., & Jump, E. (1962). The miniature pig as an experimental animal in dental research. Archives of Oral Biology, 7(1), 17-IN6.
- Wescott, K. L., & Brandon, R. J. (Eds.). (2004). Practical applications of GIS for archaeologists: A predictive modelling toolkit. CRC Press.
- Yale University, 2010. "Rwanda After the Genocide." Yale.edu. Web. <http://www.yale.edu/gsp/rwanda/rwanda_after_genocide.html>.

APPENDIX

APPENDIX I: Results for Near 3D and Osteometric Sorting

Cells highlighted in yellow indicate a correct match. Cells highlighted in red indicate an incorrect match. The cells highlighted in light blue indicate the true match if a match was incorrect. A cell containing “No match” indicates no match was found. A cell containing “*” indicates a match was found, but it has no provenience. The last column on the right titled “OS” contains the results for osteometric sorting. The number in the cell indicates how many comparisons were correctly sorted or not sorted. All distances are in meters.

Table 7.1: Left Humerus and Radius

Left Humerus and Left Radius																					
Number	LN	Age	Xi	Predicted	Formula 1	Formula 2	T-Value	P-Value	Rad 676	Rad 814	Rad 983	Rad 1393	Rad 1500	Rad 1595	Rad 1667	Rad 1909	Rad 753	Distance	Match	OS	
Hum 306	5.0876		4.79662	5.082636	0.00496	0.104432	0.047498	0.9624	0.0156	0.7000	0.0712	0.7931	0.9101	0.1132	0.0173	0.9624	0.0000	0.3745	2nd	5	
Hum 760	4.1682	Fetal	4.79662	5.082636	0.914426	0.104432	8.756142	0.0000	0.0000	0.0000	0.0000	0.0000	0.0000	0.0000	0.0000	0.0000	0.0000	0.9583	0.0985	1st	9
Hum 976	5.1795		4.79662	5.082636	0.096894	0.104432	0.927818	0.3597	0.1063	0.6251	0.3356	0.2601	0.3269	0.4636	0.1158	0.3597	0.0000	0.0492	1st	2	
Hum 1121	5.0550		4.79662	5.082636	0.027666	0.104432	0.264914	0.7926	0.0071	0.4877	0.0365	0.9620	0.8436	0.0606	0.0080	0.7926	0.0000	0.0282	1st	6	
Hum 1473	5.0460		4.79662	5.082636	0.036634	0.104432	0.350788	0.7278	0.0057	0.4364	0.0301	0.8943	0.7776	0.0506	0.0064	0.7278	0.0000	0.0162	1st	6	
Hum 1623	5.2316		4.79662	5.082636	0.149004	0.104432	1.426801	0.1623	0.2553	0.3277	0.6372	0.1092	0.1446	0.8113	0.2738	0.1623	0.0000	0.0925	1st	2	
Hum 1664	5.2751		4.79662	5.082636	0.192414	0.104432	1.842476	0.0737	0.4646	0.1676	0.9535	0.0469	0.0643	0.8610	0.4919	0.0737	0.0000	0.0442	1st	5	
Hum 1888	5.0344		4.79662	5.082636	0.048286	0.104432	0.462363	0.6466	0.0043	0.3747	0.0233	0.8076	0.6944	0.0397	0.0048	0.6466	0.0000	0.0849	1st	6	
Hum 1953	4.0792	Fetal	4.79662	5.082636	1.003406	0.104432	9.608176	0.0000	0.0000	0.0000	0.0000	0.0000	0.0000	0.0000	0.0000	0.0000	0.4606	No match	1st	0	
Hum 547	5.2653		4.79662	5.082636	0.182644	0.104432	1.748923	0.0888	0.4104	0.1969	0.8796	0.0572	0.0779	0.9347	0.4358	0.0888	0.0000	0.0845	1st	5	

Table 7.2: Left Scapula and Humerus

Left Scapula and Left Humerus																					
Number	LN	Age	Xi	Predicted	Formula 1	Formula 2	T-Value	P-Value	Hum 306	Hum 760	Hum 976	Hum 1121	Hum 1473	Hum 1623	Hum 1664	Hum 1888	Hum 1953	Hum 548	Distance	Match	OS
Scap 308	5.3399		4.78999	5.005051	0.3348888	0.2898987	1.155192	0.2563	0.8777	0.0040	0.8753	0.7920	0.7688	0.7391	0.6316	0.7391	0.0021	0.6551	0.2118	1st	3
Scap 575	5.5846		5.26528	5.468887	0.1157362	0.2860982	0.404533	0.6884	0.3206	0.0005	0.4909	0.2714	0.2589	0.6071	0.7128	0.2433	0.0002	0.6884	0.1145	1st	3
Scap 751	4.2905	Fetal	5.26528	5.468887	1.1784268	0.2860982	4.118959	0.0002	0.0013	0.0006	0.0018	0.0020	0.0003	0.0002	0.0002	0.0022	0.9461	0.0002	0.0779	1st	9
Scap 988	5.5053		5.26528	5.468887	0.0364432	0.2860982	0.12738	0.8994	0.4694	0.0009	0.6775	0.4057	0.3892	0.8102	0.9256	0.3684	0.0005	0.8994	0.0566	1st	3
Scap 1286	5.2177		5.26528	5.468887	0.2512368	0.2860982	0.878149	0.3862	0.7877	0.0111	0.5623	0.8736	0.8975	0.4507	0.3686	0.9287	0.0059	0.3862	0.0582	1st	3
Scap 1467	5.2908		5.26528	5.468887	0.1780968	0.2860982	0.622502	0.5379	0.9870	0.0061	0.7436	0.9252	0.9012	0.6151	0.5165	0.8702	0.0032	0.5379	0.0396	1st	3
Scap 1625	5.4848		5.26528	5.468887	0.0159132	0.2860982	0.055622	0.9560	0.5137	0.0011	0.7301	0.4464	0.4288	0.8658	0.9823	0.4067	0.0006	0.9560	0.0852	1st	3
Scap 1696	5.5354		5.26528	5.468887	0.0664732	0.2860982	0.232344	0.8177	0.4088	0.0007	0.6034	0.3506	0.3356	0.7308	0.8435	0.3168	0.0004	0.8177	0.0414	1st	3
Scap 1837	5.2832		5.26528	5.468887	0.1856828	0.2860982	0.649017	0.5208	0.9661	0.0065	0.7239	0.9461	0.9220	0.5968	0.4998	0.8909	0.0034	0.5208	0.2082	1st	3
Scap 2053	4.1821	Fetal	5.26528	5.468887	1.2867868	0.2860982	4.49771	0.0001	0.0005	0.4830	0.0002	0.0006	0.0007	0.0001	0.0001	0.0008	0.6769	0.0001	1.0175	5th	9

Table 7.3: Right Scapula and Humerus

Right Scapula and Right Humerus																				
Number	LN	Age	Xi	Predicted	Formula 1	Formula 2	T-Value	P-Value	Hum 377	Hum 627	Hum 655	Hum 1015	Hum 1220	Hum 1461	Hum 1478	Hum 1685	Hum 1806	Distance	Match	OS
Scap 299	5.3495		5.02388	5.233304	0.116186	0.287183	0.40457	0.6884	0.7732	0.6415	0.0037	0.8745	0.7422	0.7209	0.7329	0.6306	0.6884	0.2436	1st	2
Scap 624	5.6018		5.02388	5.233304	0.368446	0.287183	1.282964	0.2084	0.2505	0.6831	0.0004	0.4753	0.2346	0.2241	0.5946	0.6944	0.2084	0.0591	1st	2
Scap 684	4.3464	Fetal	5.02388	5.233304	0.886904	0.287183	3.088291	0.0041	0.0030	0.0004	0.8698	0.0009	0.0033	0.0036	0.0005	0.0003	0.0041	0.0646	1st	9
Scap 1010	5.5314		5.02388	5.233304	0.298106	0.287183	1.038033	0.3068	0.3619	0.8692	0.0007	0.6370	0.3413	0.3275	0.7724	0.8813	0.3068	0.0565	1st	2
Scap 1202	5.2117		5.02388	5.233304	0.021634	0.287183	0.075333	0.9404	0.8507	0.3482	0.0116	0.5262	0.8829	0.9054	0.4148	0.3405	0.9404	0.1453	1st	2
Scap 1489	5.2903		5.02388	5.233304	0.056981	0.287183	0.198412	0.8439	0.9334	0.5032	0.0061	0.7167	0.9009	0.8785	0.5852	0.4936	0.8439	0.0342	1st	2
Scap 1515	5.4914		5.02388	5.233304	0.258136	0.287183	0.898854	0.3752	0.4379	0.9792	0.0011	0.7384	0.4145	0.3989	0.8802	0.9915	0.3752	0.0176	1st	2
Scap 1644	4.1972	Fetal	5.02388	5.233304	1.036104	0.287183	3.60782	0.0010	0.0007	0.0001	0.5171	0.0002	0.0008	0.0009	0.0001	0.0001	0.0010	0.3818	No match	No match
Scap 1702	5.5424		5.02388	5.233304	0.309136	0.287183	1.076441	0.2895	0.3425	0.8392	0.0007	0.6101	0.3227	0.3094	0.7434	0.8512	0.2895	0.0177	1st	2
Scap 1779	5.2781		5.02388	5.233304	0.044816	0.287183	0.156052	0.8769	0.9669	0.4770	0.0067	0.6856	0.9343	0.9118	0.5568	0.4676	0.8769	0.0441	1st	2

Table 7.4: Left Ulna and Humerus

Left Ulna and Left Humerus																					
Number	LN	Age	Xi	Predicted	Formula 1	Formula 2	T-Value	P-Value	Hum 306	Hum 760	Hum 976	Hum 1121	Hum 1473	Hum 1623	Hum 1664	Hum 1888	Hum 1953	Hum 547	Distance	Match	OS
Uln 553	4.6151		5.26528	4.867929	0.252809	0.063868	3.958286	0.0003	0.3343	0.0000	0.0163	0.6678	0.7789	0.0017	0.0002	0.9303	0.0000	0.0003	0.2317	2nd	7
Uln 718	4.8402		5.26528	4.867929	0.027689	0.063868	0.433535	0.6672	0.0156	0.0000	0.3226	0.0039	0.0026	0.8971	0.5541	0.0015	0.0000	0.6672	0.2256	2nd	7
Uln 869	3.4657	Fetal	5.26528	4.867929	1.402193	0.063868	21.95443	0.0000	0.0000	0.0018	0.0000	0.0000	0.0000	0.0000	0.0000	0.0000	0.0598	0.0000	0.1452	1st	9
Uln 978	4.7493		5.26528	4.867929	0.118659	0.063868	1.857872	0.0714	0.2712	0.0000	0.6765	0.1052	0.0784	0.2039	0.0507	0.0525	0.0000	0.0714	0.1067	1st	7
Uln 1395	4.4942		5.26528	4.867929	0.373689	0.063868	5.85093	0.0000	0.0069	0.0000	0.0001	0.0261	0.0367	0.0000	0.0000	0.0560	0.0000	0.0000	0.0792	1st	9
Uln 1506	4.5380		5.26528	4.867929	0.329969	0.063868	5.166397	0.0000	0.0355	0.0000	0.0007	0.1102	0.1456	0.0001	0.0000	0.2045	0.0000	0.0000	0.0467	1st	8
Uln 1589	4.8203		5.26528	4.867929	0.047649	0.063868	0.746053	0.4605	0.0323	0.0000	0.4943	0.0088	0.0060	0.8564	0.3690	0.0036	0.0000	0.4605	0.0443	1st	7
Uln1609	4.7185		5.26528	4.867929	0.149429	0.063868	2.339644	0.0250	0.5284	0.0000	0.3730	0.2452	0.1915	0.0842	0.0170	0.1359	0.0000	0.0250	0.1493	1st	4
Uln 2027	4.4998		5.26528	4.867929	0.368119	0.063868	5.763719	0.0000	0.0086	0.0000	0.0001	0.0318	0.0444	0.0000	0.0000	0.0671	0.0000	0.0000	0.1192	1st	9

Table 7.5: Right Ulna and Humerus

Right Ulna and Right Humerus																				
Number	LN	Age	Xi	Predicted	Formula 1	Formula 2	T-Value	P-Value	Hum 377	Hum 627	Hum 655	Hum 1015	Hum 1220	Hum 1461	Hum 1478	Hum 1685	Hum 1806	Distance	Match	OS
Uln 640	4.8203		4.80648	4.376876	0.4434045	0.0646	6.863856	0.0000	0.0098	0.3218	0.0000	0.6051	0.0006	0.0041	0.7010	0.2871	0.0023	0.0595	1st	1
Uln 852	4.6102		4.80648	4.376876	0.2332845	0.0646	3.61122	0.0009	0.5840	0.0001	0.0000	0.0089	0.7287	0.8357	0.0008	0.0001	0.9926	0.3013	2nd	6
Uln 933	3.6109	Fetal	4.80648	4.376876	0.7659555	0.0646	11.85691	0.0000	0.0000	0.0000	0.2384	0.0000	0.0000	0.0000	0.0000	0.0000	0.0000	0.3423	2d	9
Uln 1024	4.7406		4.80648	4.376876	0.3636945	0.0646	5.629953	0.0000	0.1465	0.0305	0.0000	0.4726	0.1004	0.0761	0.1108	0.0256	0.0483	0.0677	1st	6
Uln 1271	4.4886		4.80648	4.376876	0.1117645	0.0646	1.730102	0.0922	0.0193	0.0000	0.0000	0.0000	0.0309	0.0423	0.0000	0.0000	0.0673	0.0967	1st	8
Uln 1455	4.5380		4.80648	4.376876	0.1610845	0.0646	2.493571	0.0174	0.1016	0.0000	0.0000	0.0004	0.1485	0.1900	0.0000	0.0000	0.2713	0.0397	1st	6
Uln 1468	4.6201		4.80648	4.376876	0.2431845	0.0646	3.764471	0.0006	0.6930	0.0002	0.0000	0.0131	0.8465	0.9569	0.0012	0.0002	0.8708	0.0403	1st	4
Uln 1683	4.8204		4.80648	4.376876	0.4435045	0.0646	6.865404	0.0000	0.0000	0.3226	0.0000	0.6041	0.0058	0.0040	0.7021	0.2878	0.0023	0.0384	1st	5
Uln 2039	4.4998		4.80648	4.376876	0.1229345	0.0646	1.903013	0.0651	0.0298	0.0000	0.0000	0.0001	0.0455	0.0614	0.0000	0.0000	0.0954	0.0510	1st	8
Uln 2064	3.4657	Fetal	4.80648	4.376876	0.9111395	0.0646	14.10435	0.0000	0.0000	0.0000	0.0019	0.0000	0.0000	0.0000	0.0000	0.0000	0.0000	0.2938	No match	9

Table 7.6: Left Femur and Tibia (matched in columns by tibia)

Left Femur and Left Tibia																			
Number	LN	Age	Xi	Predicted	Formula 1	Formula 2	T-Value	P-Value	Tib 6	Tib 135	Tib 389	Tib 968	Tib 1099	Tib 1158	Tib 1327	Tib 1863	Tib 1957	Tib 1992	
Fem 94	5.3423		5.17615		0.095516	0.021748	4.391898	0.0001	0.0000	0.0000	0.0000	0.0000	0.0000	0.0000	0.5090	0.0000	0.0000	0.0001	
Fem 175	4.9558		5.17615		0.290984	0.021748	13.37974	0.0000	0.2851	0.0000	0.0000	0.0000	0.0000	0.2970	0.0000	0.8121	0.0000	0.0000	
Fem 400	5.2423		5.17615		0.004538	0.021748	0.20868	0.8359	0.0000	0.0000	0.0000	0.0000	0.0080	0.0000	0.0000	0.0000	0.0000	0.8359	
Fem 842	3.9120	Fetal	5.17615		1.334791	0.021748	61.37497	0.0000	0.0000	0.0000	0.0000	0.0000	0.0000	0.0000	0.0000	0.0000	0.0000	0.0000	
Fem 1091	5.1733		5.17615		0.073494	0.021748	3.379342	0.0018	0.0000	0.0000	0.0000	0.0000	0.7199	0.0000	0.0000	0.0000	0.0000	0.0018	
Fem 1335	4.9836		5.17615		0.263204	0.021748	12.10239	0.0000	0.8527	0.0057	0.0000	0.0000	0.0000	0.0256	0.0000	0.1397	0.0000	0.0000	
Fem 1399	5.1812		5.17615		0.065594	0.021748	3.016093	0.0047	0.0000	0.0000	0.0000	0.0000	0.9986	0.0000	0.0000	0.0000	0.0000	0.0047	
Fem 1860	4.9416		5.17615		0.305174	0.021748	14.03221	0.0000	0.2281	0.0000	0.0000	0.0000	0.0000	0.6846	0.0000	0.6845	0.0000	0.0000	
Fem 1959	5.2549		5.17615		0.008076	0.021748	0.371324	0.7126	0.0000	0.0000	0.0000	0.0000	0.0017	0.0000	0.0000	0.0000	0.0000	0.7126	
									Distance	0.0737	0.0587	0.1015	0.2352	0.0778	0.0778	0.3523	0.0388	0.1495	0.0855
									Match	1st	1st	1st	No match	1st	1st	2nd	1st	1st	1st
									OS		7	8	8	8	6	7	7	8	8

Table 7.7: Right Femur and Right Tibia

Right Femur and Right Tibia																				
Number	LN	Age	Xi	Predicted	Formula 1	Formula 2	T-Value	P-Value	Tib 8	Tib 172	Tib 426	Tib 935	Tib 1079	Tib 1142	Tib 1331	Tib 1858	Tib 1996	Distance	Match	OS
Fem 84	5.0752		5.15329	5.22343	0.14826	0.021749	6.81677	0.0000	0.8372	0.0002	0.0000	0.0000	0.0002	0.0000	0.0000	0.0000	0.0000	0.1340	1st	9
Fem 177	4.9726		5.15329	5.22343	0.25084	0.021749	11.53326	0.0000	0.0001	0.5807	0.0000	0.0000	0.0000	0.0451	0.0000	0.5170	0.0000	0.1696	1st	8
Fem 404	5.2486		5.15329	5.22343	0.02517	0.021749	1.157303	0.2548	0.0000	0.0000	0.8766	0.0000	0.0004	0.0000	0.0000	0.0000	0.2548	0.1333	1st	8
Fem 938	3.9435	Fetal	5.15329	5.22343	1.27991	0.021749	58.84848	0.0000	0.0000	0.0000	0.0000	0.6715	0.0000	0.0000	0.0000	0.0000	0.0000	0.2166	1st	9
Fem 1075	5.1676		5.15329	5.22343	0.05579	0.021749	2.565126	0.0146	0.0001	0.0000	0.0004	0.0000	0.8826	0.0000	0.0000	0.0000	0.0146	0.2978	1st	9
Fem 1325	5.1930		5.15329	5.22343	0.03047	0.021749	1.400948	0.1698	0.0000	0.0000	0.0101	0.0000	0.1977	0.0000	0.0000	0.0000	0.1698	0.1358	1st	6
Fem 1343	4.9726		5.15329	5.22343	0.25084	0.021749	11.53326	0.0000	0.0001	0.5807	0.0000	0.0000	0.0000	0.0451	0.0000	0.5170	0.0000	0.0546	1st	6
Fem 1798	4.9416		5.15329	5.22343	0.28179	0.021749	12.9563	0.0000	0.0000	0.0000	0.0000	0.0000	0.0000	0.5126	0.0000	0.4511	0.0000	0.1940	1st	8
Fem 1966	5.2730		5.15329	5.22343	0.04957	0.021749	2.279163	0.0287	0.0000	0.0000	0.3407	0.0000	0.0000	0.0000	0.0000	0.0000	0.0287	0.0387	1st	7

Table 7.8: Left Tibia and Fibula

Left Tibia and Left Fibula																				
Number	LN	Age	Xi	Predicted	Formula 1	Formula 2	T-Value	P-Value	Fib 112	Fib 137	Fib 391	Fib 875	Fib 1103	Fib 1176	Fib 1406	Fib 1849	Fib 1971	Distance	Match	OS
Tib 6	4.9149		4.74927	5.100688	0.185828	0.0603681	3.078241	0.0038	0.0522	0.9762	0.0045	0.0000	0.0706	0.0680	0.0816	0.0379	0.0038	0.0472	1st	7
Tib 135	4.9816		4.74927	5.100688	0.119138	0.0603681	1.973519	0.0554	0.0036	0.2905	0.0636	0.0000	0.4556	0.0050	0.4987	0.0024	0.0554	0.0523	1st	7
Tib 389	5.3776		4.74927	5.100688	0.276902	0.0603681	4.586899	0.0000	0.0000	0.0000	0.0000	0.0000	0.0000	0.0000	0.0000	0.0000	0.0000	0.0226	1st	8
Tib 968	4.1109	Fetal	4.74927	5.100688	0.989818	0.0603681	16.39637	0.0000	0.0000	0.0000	0.0000	0.0059	0.0000	0.0000	0.0000	0.0000	0.0000	0.2143	1st	8
Tib 1099	5.1120		4.74927	5.100688	0.011302	0.0603681	0.187225	0.8524	0.0000	0.0025	0.8020	0.0000	0.1676	0.0000	0.1478	0.0000	0.8524	0.0293	1st	6
Tib 1158	4.8691		4.74927	5.100688	0.231618	0.0603681	3.836755	0.0004	0.2192	0.4364	0.0005	0.0000	0.0125	0.2684	0.0149	0.1711	0.0004	0.0396	1st	6
Tib 1327	5.2837		4.74927	5.100688	0.183022	0.0603681	3.031773	0.0043	0.0000	0.0000	0.0036	0.0000	0.0001	0.0000	0.0000	0.0043	0.0452	1st	8	
Tib 1863	4.8866		4.74927	5.100688	0.214108	0.0603681	3.546701	0.0010	0.1323	0.6219	0.0012	0.0000	0.0252	0.1662	0.0297	0.1004	0.0010	0.2263	1st	6
Tib 1957	3.7495	Fetal	4.74927	5.100688	1.351188	0.0603681	22.38248	0.0000	0.0000	0.0000	0.0000	0.0116	0.0000	0.0000	0.0000	0.0000	0.0000	*	*	*
Tib 1992	5.1762		4.74927	5.100688	0.075462	0.0603681	1.250038	0.2185	0.0000	0.0001	0.1959	0.0000	0.0180	0.0000	0.0152	0.0000	0.2185	0.0552	1st	8

Table 7.9: Right Tibia and Fibula

Right Tibia and Right Fibula																				
Number	LN	Age	Xi	Predicted	Formula 1	Formula 2	T-Value	P-Value	Fib 82	Fib 170	Fib 428	Fib 862	Fib 1083	Fib 1148	Fib 1323	Fib 1819	Fib 2086	Distance	Match	OS
Tib 8	5.0040		4.74927	5.100688	0.096738	0.0603681	1.602462	0.1169	0.1909	0.0018	0.1023	0.0000	0.7040	0.0023	0.9793	0.0008	0.1169	0.0605	1st	5
Tib 172	4.9200		4.74927	5.100688	0.180708	0.0603681	2.993428	0.0047	0.9554	0.0570	0.0039	0.0000	0.0839	0.0687	0.1647	0.0314	0.0047	0.0158	1st	6
Tib 426	5.1812		4.74927	5.100688	0.080532	0.0603681	1.334022	0.1897	0.0001	0.0000	0.2134	0.0000	0.0147	0.0000	0.0059	0.0000	0.1897	0.0525	1st	8
Tib 935	3.9120	Fetal	4.74927	5.100688	1.188668	0.0603681	19.69033	0.0000	0.0000	0.0000	0.0000	0.7140	0.0000	0.0000	0.0000	0.0000	0.0000	0.2903	2nd	9
Tib 1079	5.0956		4.74927	5.100688	0.005098	0.0603681	0.084442	0.9331	0.0070	0.0000	0.8784	0.0000	0.2635	0.0000	0.1440	0.0000	0.9331	0.0470	1st	6
Tib 1142	4.8637		4.74927	5.100688	0.237008	0.0603681	3.92604	0.0003	0.3300	0.3075	0.0003	0.0000	0.0100	0.3508	0.0240	0.1993	0.0003	0.0636	1st	6
Tib 1331	5.3186		4.74927	5.100688	0.217922	0.0603681	3.609893	0.0008	0.0000	0.0000	0.0010	0.0000	0.0000	0.0000	0.0000	0.0000	0.0008	0.1211	1st	8
Tib 1858	4.8941		4.74927	5.100688	0.206588	0.0603681	3.422132	0.0014	0.6312	0.1329	0.0012	0.0000	0.0336	0.1563	0.0726	0.0786	0.0014	0.0428	1st	5
Tib 1996	5.1533		4.74927	5.100688	0.052602	0.0603681	0.871361	0.3888	0.0005	0.0000	0.4274	0.0000	0.0431	0.0000	0.0190	0.0000	0.3888	0.1269	1st	8

Table 7.10 Right Talus and Right Calcaneus

Right Talus and Right Calcaneus																				
Number	LN	Age	Xi	Predicted	Formula 1	Formula 2	T-Value	P-Value	Cal 96	Cal 168	Cal 433	Cal 909	Cal 1093	Cal 1155	Cal 1174	Cal 2003	Cal 2032	Distance	Match	OS
Tal 97	4.3833		3.8712	4.17792	0.20536	1.695869	0.1211	0.9042	0.9352	0.9316	0.9589	0.7574	0.9505	0.9589	0.9493	0.9565	0.9042	0.0507	1st	1
Tal 169	4.2808		3.8712	4.17792	0.102904	1.695869	0.0607	0.9519	0.9830	0.9795	0.9933	0.8011	0.9984	0.9933	0.9972	0.9956	0.9519	0.0154	1st	1
Tal 432	4.5207		3.8712	4.17792	0.34278	1.695869	0.2021	0.8409	0.8714	0.8679	0.8949	0.7000	0.8866	0.8949	0.8854	0.8926	0.8409	0.0536	1st	1
Tal 1090	4.4909		3.8712	4.17792	0.31296	1.695869	0.1845	0.8545	0.8851	0.8816	0.9088	0.7123	0.9004	0.9088	0.8992	0.9064	0.8545	0.1062	1st	1
Tal 1150	4.3281		3.8712	4.17792	0.15018	1.695869	0.0886	0.9299	0.9609	0.9574	0.9846	0.7808	0.9763	0.9846	0.9751	0.9823	0.9299	0.0591	1st	1
Tal 1210	4.5087		3.8712	4.17792	0.330739	1.695869	0.1950	0.8464	0.8769	0.8734	0.9005	0.7050	0.8922	0.9005	0.8910	0.8982	0.8464	0.0728	1st	1
Tal 1814	4.3241		3.8712	4.17792	0.14621	1.695869	0.0862	0.9317	0.9628	0.9592	0.9865	0.7825	0.9782	0.9865	0.9769	0.9842	0.9317	0.1001	1st	1
Tal 1999	4.5747		3.8712	4.17792	0.39678	1.695869	0.2340	0.8162	0.8465	0.8430	0.8700	0.6779	0.8617	0.8700	0.8605	0.8676	0.8162	0.0292	1st	1

Table 7.11: Left Talus and Calcaneus

Left Talus and Left Calcaneus																				
Number	LN	Age	Xi	Predicted	Formula 1	Formula 2	T-Value	P-Value	Cal 116	Cal 129	Cal 385	Cal 1052	Cal 1107	Cal 1160	Cal 1215	Cal 2009	Cal 2052	Distance	Match	Os
Tal 115	4.2753		2.8332	3.828322	0.446958	1.783748	0.2506	0.8035	0.9577	0.9787	0.9930	0.9609	0.9973	0.9671	0.9973	0.9918	0.8035	0.0273	1st	1
Tal 128	4.3656		2.8332	3.828322	0.537318	1.783748	0.3012	0.7648	0.9156	0.9365	0.9648	0.9188	0.9551	0.9249	0.9605	0.9659	0.7648	0.0324	1st	1
Tal 369	4.2929		2.8332	3.828322	0.464598	1.783748	0.2605	0.7959	0.9495	0.9705	0.9987	0.9527	0.9890	0.9588	0.9945	0.9999	0.7959	0.1279	1st	1
Tal 1105	4.4785		2.8332	3.828322	0.650148	1.783748	0.3645	0.7175	0.8634	0.8841	0.9122	0.8665	0.9025	0.8726	0.9079	0.9134	0.7175	0.0399	1st	1
Tal 1144	4.3188		2.8332	3.828322	0.490498	1.783748	0.2750	0.7848	0.9374	0.9584	0.9866	0.9406	0.9769	0.9467	0.9823	0.9878	0.7848	0.2087	1st	1
Tal 1330	4.4920		2.8332	3.828322	0.663679	1.783748	0.3721	0.7119	0.8572	0.8778	0.9059	0.8603	0.8962	0.8663	0.9016	0.9071	0.7119	0.1081	1st	1
Tal 1868	4.3307		2.8332	3.828322	0.502408	1.783748	0.2817	0.7797	0.9319	0.9528	0.9811	0.9350	0.9714	0.9412	0.9768	0.9822	0.7797	0.0640	1st	1
Tal 2010	4.5901		2.8332	3.828322	0.761738	1.783748	0.4270	0.6717	0.8124	0.8327	0.8606	0.8154	0.8509	0.8214	0.8563	0.8617	0.6717	0.0195	1st	1

7.12: Left Tibia and Talus

Left Tibia and Left Talus																			
Number	LN	Age	Xi	Predicted	Formula 1	Formula 2	T-Value	P-Value	115	128	369	1105	1144	1330	1868	2010	Distance	Match	OS
Tib 6	4.9149		4.21951	5.189207	0.274347	0.945587	0.290134	0.7734	0.7169	0.6297	0.6995	0.5304	0.6742	0.5193	0.6627	0.4442	0.0751	1st	1
Tib 135	4.9816		4.21951	5.189207	0.207657	0.945587	0.219606	0.8274	0.7698	0.6800	0.7518	0.5765	0.7259	0.5648	0.7140	0.4856	0.0263	1st	1
Tib 389	5.3776		4.21951	5.189207	0.188383	0.945587	0.199223	0.8432	0.9020	0.9983	0.9207	0.8826	0.9484	0.8686	0.9611	0.7701	0.0415	1st	1
Tib 968	4.1109	Fetal	4.21951	5.189207	1.078337	0.945587	1.140389	0.2617	0.2320	0.1903	0.2232	0.1486	0.2109	0.1443	0.2055	0.1150	0.3738	No match	
Tib 1099	5.1120		4.21951	5.189207	0.077217	0.945587	0.08166	0.9354	0.8762	0.7824	0.8570	0.6719	0.8306	0.6593	0.8182	0.5726	0.0407	1st	1
Tib 1158	4.8691		4.21951	5.189207	0.320137	0.945587	0.338559	0.7369	0.6814	0.5962	0.6643	0.4999	0.6396	0.4829	0.6280	0.4170	0.1023	1st	1
Tib 1327	5.2837		4.21951	5.189207	0.094503	0.945587	0.099941	0.9209	0.9804	0.9233	0.9993	0.8062	0.9731	0.7926	0.9604	0.6976	0.1312	1st	1
Tib 1863	4.8866		4.21951	5.189207	0.302627	0.945587	0.320041	0.7508	0.6949	0.6089	0.6777	0.5114	0.6527	0.5006	0.6414	0.4273	0.0479	1st	1
Tib 1957	3.7495	Fetal	4.21951	5.189207	1.439707	0.945587	1.522554	0.1366	0.1188	0.0947	0.1136	0.0719	0.1065	0.0696	0.1034	0.0553	0.3422	No match	
Tib 1992	5.1762		4.21951	5.189207	0.013057	0.945587	0.013808	0.9891	0.9295	0.8345	0.9108	0.7211	0.9295	0.7081	0.8709	0.6180	0.0260	1st	1

7.13: Right Tibia and Talus

Right Tibia and Right Talus																			
Number	LN	Age	Xi	Predicted	Formula 1	Formula 2	T-Value	P-Value	Tal 97	Tal 169	Tal 432	Tal 1090	Tal 1150	Tal 1210	Tal 1814	Tal 1999	Distance	Match	OS
Tib 8	5.0040		4.5747	5.642287	0.638337	0.963816	0.662302	0.5120	0.6801	0.7821	0.5560	0.5815	0.7342	0.5662	0.7382	0.5120	0.0335		1
Tib 172	4.9200		4.5747	5.642287	0.722307	0.963816	0.749424	0.4585	0.6172	0.7154	0.4996	0.5236	0.6691	0.5092	0.6730	0.4585	0.0273		1
Tib 426	5.1812		4.5747	5.642287	0.461067	0.963816	0.478377	0.6353	0.8204	0.9279	0.6847	0.7131	0.8778	0.6961	0.8820	0.6353	0.0216		1
Tib 935	3.9120	Fetal	4.5747	5.642287	1.730267	0.963816	1.795225	0.0810	0.1259	0.1603	0.0915	0.0979	0.1434	0.0940	0.1447	0.0810		No match	
Tib 1079	5.0956		4.5747	5.642287	0.546697	0.963816	0.567222	0.5741	0.7516	0.8568	0.6210	0.6481	0.8076	0.6319	0.8117	0.5741	0.1501		1
Tib 1142	4.8637		4.5747	5.642287	0.778607	0.963816	0.807838	0.4245	0.5766	0.6719	0.4637	0.4866	0.6268	0.4728	0.6306	0.4245	0.0203		1
Tib 1331	5.3186		4.5747	5.642287	0.323677	0.963816	0.335829	0.7389	0.9337	0.9571	0.7918	0.8218	0.9924	0.8039	0.9966	0.7389	0.0224		1
Tib 1858	4.8941		4.5747	5.642287	0.748187	0.963816	0.776276	0.4427	0.5984	0.6953	0.4829	0.5064	0.6495	0.4923	0.6533	0.4427	0.1366		1
Tib 1996	5.1533		4.5747	5.642287	0.488997	0.963816	0.507355	0.6150	0.7978	0.9046	0.6637	0.6916	0.8548	0.6749	0.8589	0.6150	0.0173		1

7.14: Left Femur and Ilium

Left Femur and Left Ilium																					
Number	LN	Age	Xi	Predicted	Formula 1	Formula 2	T-Value	P-Value	Ili 86	Ili 182	Ili 411	Ili 667	Ili 1077	Ili 1333	Ili 1402	Ili 1812	Ili 1900	Ili 2050	Distance	Match	OS
Fem 94	5.3423		2.77259	3.503177	1.839153	0.3952405	4.6533	0.0001	0.1766	0.0840	0.4825	0.0001	0.3066	0.0691	0.3332	0.7414	0.4062	0.0001	0.0975	1st	4
Fem 175	4.9558		2.77259	3.503177	1.452653	0.3952405	3.6754	0.0010	0.8000	0.5093	0.6749	0.0019	0.9267	0.4480	0.8819	0.3853	0.7724	0.0010	0.0554	1st	3
Fem 400	5.2423		2.77259	3.503177	1.739099	0.3952405	4.4001	0.0001	0.2835	0.1445	0.6793	0.0003	0.4608	0.1207	0.4953	0.6243	0.5871	0.0001	0.1787	1st	3
Fem 842	3.9120	Fetal	2.77259	3.503177	0.408846	0.3952405	1.0344	0.3098	0.0092	0.0252	0.0016	0.4669	0.0038	0.0319	0.0033	0.9974	0.0023	0.3098	0.2897	2nd	8
Fem 1091	5.1733		2.77259	3.503177	1.670143	0.3952405	4.2256	0.0002	0.3800	0.2040	0.8312	0.0004	0.5898	0.1724	0.6290	0.5345	0.7313	0.0002	0.0795	1st	3
Fem 1335	4.9836		2.77259	3.503177	1.480433	0.3952405	3.7457	0.0008	0.7386	0.4600	0.7347	0.0016	0.9911	0.4025	0.9460	0.3523	0.8349	0.0008	0.1046	1st	3
Fem 1399	5.1812		2.77259	3.503177	1.678043	0.3952405	4.2456	0.0002	0.3680	0.1963	0.8133	0.0004	0.5742	0.1657	0.6129	0.5449	0.7141	0.0002	0.0779	1st	3
Fem 1860	4.9416		2.77259	3.503177	1.438463	0.3952405	3.6395	0.0011	0.8319	0.5356	0.6451	0.0021	0.8940	0.4724	0.8495	0.4028	0.7411	0.0011	0.1571	1st	3
Fem 1959	5.2549		2.77259	3.503177	1.751713	0.3952405	4.4320	0.0001	0.2679	0.1353	0.6527	0.0002	0.4392	0.1128	0.4727	0.6401	0.5623	0.0001	0.1882	1st	3

7.15: Right Femur and Ilium

Right Femur and Right Ilium																					
Number	LN	Age	Xi	Predicted	Formula 1	Formula 2	T-Value	P-Value	Ili 88	Ili 180	Ili 460	Ili 517	Ili 669	Ili 1320	Ili 1341	Ili 1824	Ili 1965	Ili 1968	Distance	Match	OS
Fem 84	5.0752		2.83321	3.56356	1.51161	0.3915192	3.860882	0.0006	0.5412	0.3536	0.9133	0.7925	0.0009	0.8582	0.2695	0.3042	0.9232	0.0006	0.1212	1st	3
Fem 177	4.9726		2.83321	3.56356	1.40903	0.3915192	3.598877	0.0012	0.7523	0.5243	0.6840	0.9720	0.0017	0.9047	0.4141	0.4602	0.8398	0.0012	0.0649	1st	3
Fem 404	5.2486		2.83321	3.56356	1.68504	0.3915192	4.303849	0.0002	0.2698	0.1587	0.6923	0.4451	0.0003	0.4962	0.1144	0.1322	0.5490	0.0002	0.1482	1st	3
Fem 938	3.9435	Fetal	2.83321	3.56356	0.37996	0.3915192	0.970475	0.3401	0.0119	0.0260	0.0019	0.0049	0.4274	0.0039	0.0399	0.0332	0.0032	0.3401	0.3975	2nd	9
Fem 1075	5.1676		2.83321	3.56356	1.60408	0.3915192	4.097065	0.0003	0.3816	0.2355	0.8725	0.5955	0.0005	0.6549	0.1741	0.1991	0.7150	0.0003	0.1473	1st	3
Fem 1325	5.1930		2.83321	3.56356	1.6294	0.3915192	4.161736	0.0003	0.3437	0.2090	0.8149	0.5460	0.0004	0.6030	0.1532	0.1758	0.6610	0.0003	0.0717	1st	3
Fem 1343	4.9726		2.83321	3.56356	1.40903	0.3915192	3.598877	0.0012	0.7523	0.5243	0.6840	0.9720	0.0017	0.9047	0.4141	0.4602	0.8398	0.0012	0.0556	1st	3
Fem 1798	4.9416		2.83321	3.56356	1.37808	0.3915192	3.519826	0.0015	0.8212	0.5835	0.6194	0.9005	0.0021	0.8338	0.4659	0.5154	0.7702	0.0015	0.0396	1st	3
Fem 1966	5.2730		2.83321	3.56356	1.709439	0.3915192	4.366169	0.0002	0.2413	0.1400	0.6409	0.4047	0.0002	0.4530	0.1002	0.1161	0.5032	0.0002	0.0290	1st	3